EUROPEAN ORGANIZATION FOR PARTICLE PHYSICS

CERN-PPE/95-172
24 November 1995

A Combination of Preliminary LEP Electroweak Measurements and Constraints on the Standard Model*

The LEP Collaborations ALEPH, DELPHI, L3, OPAL and the LEP Electroweak Working Group†

Prepared from Contributions of the LEP Experiments to the 1995 International Europhysics Conference on High-Energy Physics, 27/7 to 2/8/1995, Brussels, Belgium and the 17th International Symposium on Lepton-Photon Interactions, 10-15/8/1995, Beijing, China.

Abstract

This note presents a combination of published and preliminary electroweak results from the four LEP collaborations which were prepared for the 1995 summer conferences. Averages of LEP results concerning electroweak physics are presented. They are derived from the measurements of hadronic and leptonic cross sections, the leptonic forward-backward asymmetries, the τ polarization asymmetries, the $b\overline{b}$ and $c\overline{c}$ partial widths and forward-backward asymmetries and the $q\overline{q}$ charge asymmetry. The LEP results are compared to precise electroweak measurements from other experiments. The parameters of the Standard Model are evaluated, first using the combined LEP electroweak measurements, and then using the full set of precise electroweak results. For the first time the LEP and SLD heavy flavour results are combined in a consistent manner with the help of members of the SLD collaboration.

*The LEP Collaborations each take responsibility for the preliminary data of their own experiments.

†The present members of the LEP Electroweak Working Group are: P. Antilogus, T. Behnke, D. Bloch, A. Blondel, I. Brock, J. Busenitz, D.G. Charlton, R. Clare, P. Clarke, S. Ganguli, M.W. Grünewald, A. Gurtu, R.W.L. Jones, A. Kounine, M. Mannelli, M. Martinez, K. Mönig, G. Myatt, A. Olshevsky, A. Passeri, Ch. Paus, M. Pepe-Altarelli, P. Perret, B. Pietrzyk, P. Renton, D. Reid, M. Roney, D. Schaile, D. Schlatter, T.J. Smith, R. Tenchini, F. Teubert, P.S. Wells.

1 Introduction

In a recent note [1] the four LEP experiments have presented parameters derived from the Z resonance using published and preliminary results based on data recorded until the end of 1993. The preliminary results were contributions to the 27th International Conference on High-Energy Physics, Glasgow, Scotland, 20-27 July 1994.

Since then several analyses have been completed and published. The calibration of the LEP energy scale for the high-statistics scan of the Z resonance in 1993 has been finalized [2], resulting in a reduction of errors on the Z mass, m_{Z}, and total width, Γ_{Z}, due to the uncertainties in the LEP centre-of-mass energy.

Furthermore several new preliminary results from the 1994 running period have become available. In 1994 the LEP experiments approximately doubled their event statistics. Important progress has also been achieved for the theoretical error associated with the luminosity determination [3]. It is expected that an even better theoretical precision will finally be obtained. The interpretation of electroweak precision data requires a precise knowledge of the fine structure constant evaluated at the Z pole, $\alpha(m_{\mathrm{Z}}^2)$, for which several reevaluations have been performed recently [4–7]. Last but not least, the CDF and DØ collaborations have published their discovery of the top quark [8,9].

The data consist of the hadronic and leptonic cross sections, the leptonic forward-backward asymmetries, the τ polarization asymmetries, the $\mathrm{b\overline{b}}$ and $\mathrm{c\overline{c}}$ partial widths and forward-backward asymmetries and the $\mathrm{q\overline{q}}$ charge asymmetry. Many technical aspects of their combination have already been described in [1] and references therein. It should be stressed, however, that several measurements included in the current combination as well as the procedure for averaging the heavy-flavour results are still preliminary.

This note is organized in the following manner. In Section 2 the results on the Z line shape and leptonic forward-backward asymmetries are presented, while Section 3 contains the measurements of the τ polarization. Section 4 describes the parameters resulting from heavy flavour analyses, Section 5 new results for the inclusive hadronic charge asymmetry. Section 6 is devoted to the interpretation of the results. In Sections 6.1, 6.2 and 6.3 several LEP electroweak measurements are combined to determine the effective neutral current coupling constants and to give a value of the effective electroweak mixing angle. We also quote values for these parameters when the left-right and left-right forward-backward asymmetries from SLD [10–12] are included. The determination of the number of light neutrino species is discussed in Section 6.4. In Section 6.5 the LEP data and also data from SLD [10–13], from neutrino interactions [14–16] and from measurements of the mass of the W boson [17–20] and the top quark [8,9] are used to constrain the parameters of the Standard Model.

2 Z Lineshape and Lepton Forward-Backward Asymmetries

The results presented here are based on the data taken during the energy scans in 1990 and 1991 with centre-of-mass energies, $\sqrt{s}$, in a range $|\sqrt{s} - m_{\mathrm{Z}}| < 3$ GeV, on the data collected at the Z peak in 1992 and on a preliminary analysis of the energy scan in 1993. During 1993 more than 18 pb^{-1} were recorded by each experiment at two centre-of-mass energy points roughly 1.8 GeV above and below the Z mass, while about 15 pb^{-1} were within 200 MeV of m_{Z}. We also add several preliminary results based on data of the 1994 running period where the LEP experiments each collected approximately 55 pb^{-1} at the Z peak.

The total statistics and the systematic errors on the individual analyses of the four LEP collaborations are given in Tables 1 and 2. Details of the individual analyses can be found in References 21–24. An important aspect of the lineshape analysis is a precise knowledge of the LEP centre-of-mass energies. The treatment of the LEP centre-of-mass energies by the four LEP experiments is based on [2]. For the 1994 data a preliminary LEP energy calibration is available [25]. In combining all of the recorded data, the energy uncertainty from the 1993 data and from the data of previous years is taken to be uncorrelated.

The errors corresponding to the LEP energy uncertainty are estimated by an approximate method. Fits are performed to the data from a single experiment with all error components, other than those from the LEP energy, reduced so that they correspond approximately to those of the four experiments combined. Comparison with the usual fits then allows the error components due to the LEP energy uncertainty to be extracted. The result of this procedure is insensitive to which of the experiments is used in such a fit.

For the averaging of results the LEP experiments provide a standard set of 9 parameters describing the information contained in hadronic and leptonic cross sections and leptonic forward-backward asymmetries [1, 26]. These parameters have initial-state QED corrections, as well as t-channel and s/t-interference contributions in the case of the e^+e^- final state, removed. They are convenient for fitting and averaging since they have small correlations. The parameters are:

- The mass and total width of the Z boson, where the definition is based on the Breit-Wigner denominator $(s - m_Z^2 + is\Gamma_Z/m_Z)$ [27].

- The hadronic pole cross section of Z exchange:

$$\sigma_h^0 \equiv \frac{12\pi}{m_Z^2}\frac{\Gamma_{ee}\Gamma_{had}}{\Gamma_Z^2}\,.$$

  Here Γ_{ee} and Γ_{had} are the partial widths of the Z for decays into electrons and hadrons.

- The ratios:

$$R_e \equiv \Gamma_{had}/\Gamma_{ee} \qquad R_\mu \equiv \Gamma_{had}/\Gamma_{\mu\mu} \qquad R_\tau \equiv \Gamma_{had}/\Gamma_{\tau\tau}. \tag{1}$$

  Here $\Gamma_{\mu\mu}$ and $\Gamma_{\tau\tau}$ are the partial widths of the Z for the decays $Z \to \mu^+\mu^-$ and $Z \to \tau^+\tau^-$. Even under the assumption of lepton universality a small difference of 0.2% is expected between the values for R_e and R_μ, and the value for R_τ, owing to mass corrections to $\Gamma_{\tau\tau}$.

- The pole asymmetries, $A_{FB}^{0,e}$, $A_{FB}^{0,\mu}$ and $A_{FB}^{0,\tau}$ for the processes $e^+e^- \to e^+e^-$, $e^+e^- \to \mu^+\mu^-$ and $e^+e^- \to \tau^+\tau^-$. In terms of the effective vector and axial-vector neutral current couplings of fermions, g_{Vf} and g_{Af}, the pole asymmetries are expressed as:[1]

$$A_{FB}^{0,f} \equiv \frac{3}{4}\mathcal{A}_e\mathcal{A}_f \tag{2}$$

  with:

$$\mathcal{A}_f \equiv \frac{2g_{Vf}g_{Af}}{g_{Vf}^2 + g_{Af}^2}\,. \tag{3}$$

[1] In the definition of $A_{FB}^{0,f}$, effects coming from γ exchange, γ/Z interference, as well as real and imaginary parts of the photon vacuum polarization are not included. They are accounted for explicitly in the fitting formulae used by the experiments, and are fixed to their Standard Model values.

This set of 9 parameters does not describe the Z production and decay completely, because it does not include the interference of the Z exchange with the γ exchange. This contribution is investigated in a separate note [28]. For the results presented in this Section, the γ-exchange contributions and the γZ interference terms are fixed to their Standard Model values.[2]

The four sets of 9 parameters provided by the LEP experiments are presented in Table 3. The covariance matrix of these parameters is as described in our previous paper [26]. It is constructed from the covariance matrices of the individual LEP experiments and common systematic errors. These common errors arise from the theoretical uncertainty in the luminosity normalization affecting the hadronic pole cross section, $\Delta\sigma^0_{\rm h}/\sigma^0_{\rm h} = 0.16\%$, from the uncertainty of the LEP centre-of-mass energy spread of 5 MeV [2], resulting in $\Delta\Gamma_{\rm Z} \approx 1.0$ MeV, and from the uncertainty in the LEP energy calibration. The latter uncertainty causes errors of $\Delta m_{\rm Z} \approx 1.5$ MeV, $\Delta\Gamma_{\rm Z} \approx 1.7$ MeV, and $\Delta A^{0,\ell}_{\rm FB} \approx 0.0005$ for each lepton species ($\ell = {\rm e}, \mu, \tau$). Full correlation between $A^{0,\mu}_{\rm FB}$ and $A^{0,\tau}_{\rm FB}$ and full anti-correlation between $A^{0,{\rm e}}_{\rm FB}$ and $A^{0,\mu}_{\rm FB}$ or $A^{0,\tau}_{\rm FB}$ is used. This anti-correlation for $A^{0,{\rm e}}_{\rm FB}$ is an approximation of the effect of the t-channel contribution for a typical LEP experimental acceptance for the ${\rm e^+e^-}$ final state. The combined parameter set and its correlation matrix are given in Tables 4 and 5.

If lepton universality is assumed, the set of 9 parameters given above is reduced to a set of 5 parameters. R_ℓ is defined as $R_\ell \equiv \Gamma_{\rm had}/\Gamma_{\ell\ell}$, where $\Gamma_{\ell\ell}$ refers to the partial Z width for the decay into a pair of massless charged leptons.

The data of each of the four LEP experiments are consistent with lepton universality (the difference in χ^2 over the difference in d.o.f. with and without the assumption of lepton universality are 6/4, 4/4, 4/4 and 5/4 for ALEPH, DELPHI, L3 and OPAL, respectively). Based on this assumption Table 6 provides the five parameters $m_{\rm Z}$, $\Gamma_{\rm Z}$, $\sigma^0_{\rm h}$, R_ℓ and $A^{0,\ell}_{\rm FB}$ for the individual LEP experiments. The four experiments all use the above definition of $\Gamma_{\ell\ell}$. Tables 7 and 8 provide these five parameters and the corresponding correlation matrix for the combined result of the four LEP experiments. Figure 1 shows, for each lepton species and for the combination assuming lepton universality, the resulting 68% probability contours in the R_ℓ-$A^{0,\ell}_{\rm FB}$ plane.

For completeness the partial decay widths of the Z boson are listed in Table 9. Note that the substantial improvement of $\Gamma_{\ell\ell}$ as compared to Reference 1 is essentially due to a decrease of systematic errors on both the LEP energy calibration and the theoretical calculation of the small angle Bhabha cross section.

[2] If instead the γZ interference terms are entirely determined from LEP cross-section data, the total error on the LEP average of $m_{\rm Z}$ increases from 2.2 MeV to 6.2 MeV [28].

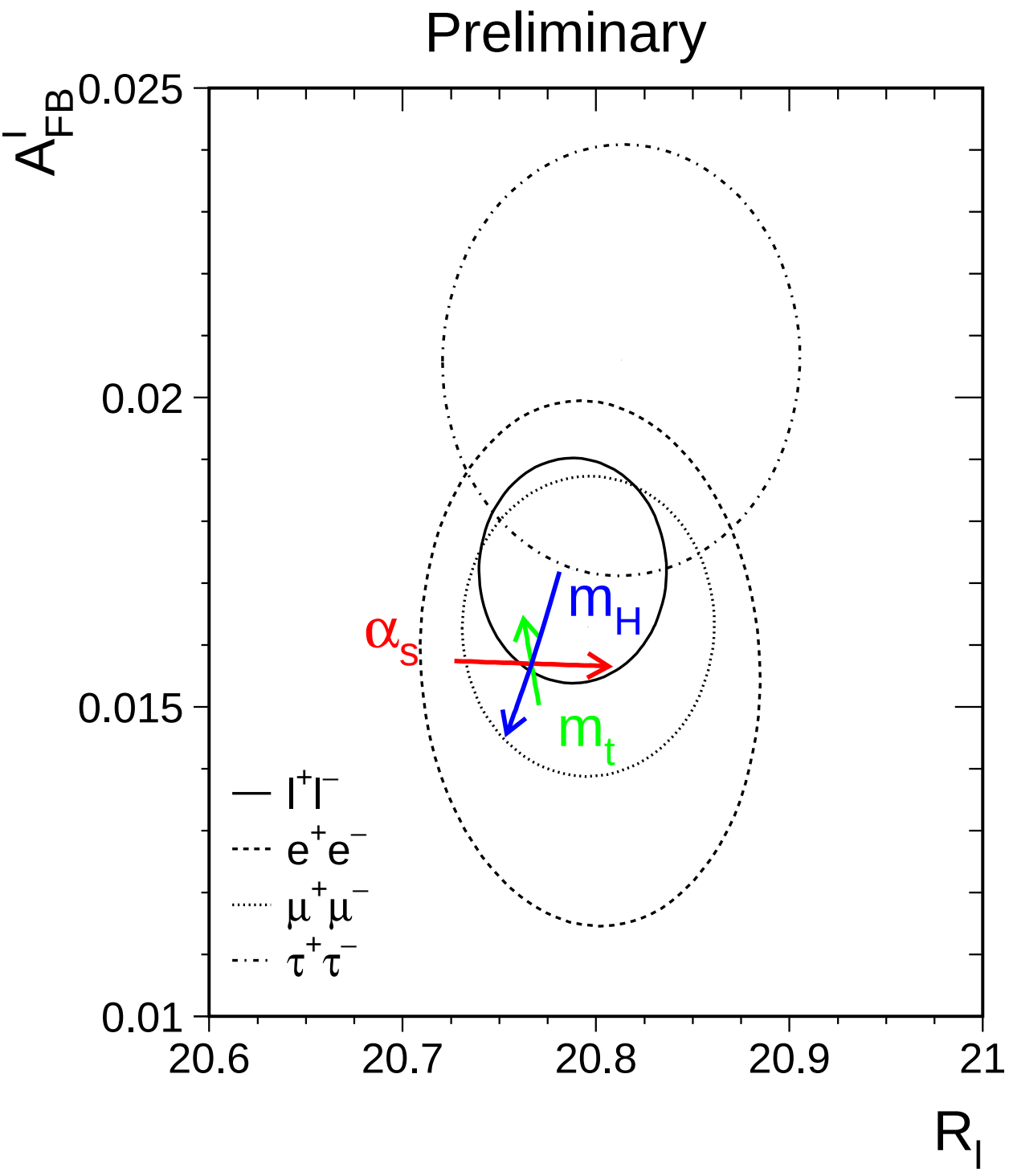

Figure 1: Contours of 68% probability in the R_ℓ-$A_{\rm FB}^{0,\ell}$ plane. The Standard Model prediction for $m_{\rm Z} = 91.1884$ GeV, $m_{\rm t} = 180$ GeV, $m_{\rm H} = 300$ GeV, and $\alpha_s = 0.123$ is also shown. The lines with arrows correspond to the variation of the Standard Model prediction when $m_{\rm t}$, $m_{\rm H}$ or $\alpha_s(m_{\rm Z}^2)$ are varied in the intervals $m_{\rm t} = 180 \pm 12$ GeV, $m_{\rm H} = 300^{+700}_{-240}$ GeV, and $\alpha_s(m_{\rm Z}^2) = 0.123 \pm 0.006$, respectively. The arrows point in the direction of increasing values of $m_{\rm t}$, $m_{\rm H}$ and α_s.

		ALEPH	DELPHI	L3	OPAL	LEP
$q\bar{q}$	'90-'91	451	356	416	454	1677
	'92	680	697	678	733	2788
	'93 prel.	640	677	654	646	2617
	'94 prel.	1281	[b]1144	1362	1524	5311
	total	3052	2874	3110	3357	12393
$\ell^+\ell^-$	'90-'91	55	37	40	58	190
	'92	82	69	58	88	297
	'93 prel.	78	71	61	82	292
	'94 prel.	[a]155	[b]54	123	184	516
	total	370	231	282	412	1295

Table 1: The LEP statistics in units of 10^3 events used for the analysis of the Z line shape and lepton forward-backward asymmetries.
[a]Statistics used in the measurement of the lepton cross section. The statistics used in the lepton forward-backward asymmetries is about 27% higher.
[b]Only part of the 1994 data set is included here. The results for leptons are for the $\mu^+\mu^-$ channel only.

	ALEPH		DELPHI		L3		OPAL	
	'93 prel.	'94 prel.	'93 prel.	'94 prel.	'93 prel.	'94 prel.	'93 prel.	'94 prel.
$\mathcal{L}^{\text{exp.}}$ [b]	0.087%	0.116%	0.21%	0.09%	0.12%	0.15%	0.076%	0.079%
σ_{had}	0.073%	0.073%	0.13%	0.15%	0.08%	0.2%	0.15%	0.16%
σ_e	0.50 %	0.48%	0.44%	[a]	0.3%	0.4%	0.23%	0.24%
σ_μ	0.25 %	0.26%	0.28%	0.40%	0.3%	0.6%	0.16%	0.15%
σ_τ	0.34 %	0.32%	0.8%	[a]	0.6%	1.5%	0.43%	0.46%
A_{FB}^e	0.003	0.003	0.0026	[a]	0.004	0.004	0.0016	0.0016
A_{FB}^μ	0.001	0.001	0.0009	0.0015	0.001	0.002	0.001	0.001
A_{FB}^τ	0.004	0.004	0.0023	[a]	0.004	0.006	0.002	0.002

Table 2: The experimental systematic errors for the analysis of the Z line shape and lepton forward-backward asymmetries at the Z peak. The errors quoted do not include the common uncertainty due to the LEP energy calibration. The treatment of correlations between the errors for different years is described in References 21–24.
[a]No preliminary result quoted yet.
[b]In addition, there is a theoretical error for the calculation of the small angle Bhabha cross section of 0.16%, which has been treated as common to all experiments. The DELPHI theoretical error for 1993 is 0.17%.

	ALEPH	DELPHI	L3	OPAL
$m_{\rm Z}$(GeV)	91.1924±0.0037	91.1849±0.0034	91.1936±0.0036	91.1852±0.0036
$\Gamma_{\rm Z}$(GeV)	2.4954±0.0057	2.4913±0.0054	2.5022±0.0054	2.4960±0.0053
$\sigma^0_{\rm h}$(nb)	41.56±0.09	41.39±0.10	41.48±0.11	41.47±0.10
R_e	20.54±0.11	20.88±0.16	20.89±0.12	20.90±0.10
R_μ	20.88±0.09	20.70±0.09	20.80±0.11	20.796±0.073
R_τ	20.77±0.10	20.61±0.16	20.73±0.17	21.00±0.11
$A^{0,\,\rm e}_{\rm FB}$	0.0196±0.0044	0.0233±0.0070	0.0125±0.0070	0.0081±0.0051
$A^{0,\,\mu}_{\rm FB}$	0.0189±0.0029	0.0166±0.0030	0.0168±0.0038	0.0137±0.0027
$A^{0,\,\tau}_{\rm FB}$	0.0206±0.0039	0.0210±0.0057	0.0287±0.0064	0.0183±0.0035
χ^2/d.o.f.	181/185	151/135	118/138	$10/6^{(a)}$

Table 3: Line shape and asymmetry parameters from 9-parameter fits to the data of the four LEP experiments.
$^{(a)}$This parameter set has been obtained from a parameter transformation applied to the 15 parameters of the OPAL fit [24], which treats the γZ interference terms for leptons as additional free parameters. The extra parameters for the γZ interference terms have been fixed to their Standard Model values in the transformation. The χ^2/d.o.f. for the 15-parameter fit to the data is 87/132.

Parameter	Average Value
$m_{\rm Z}$(GeV)	91.1885±0.0022
$\Gamma_{\rm Z}$(GeV)	2.4963±0.0032
$\sigma^0_{\rm h}$(nb)	41.488±0.078
$R_{\rm e}$	20.797±0.058
R_μ	20.796±0.043
R_τ	20.813±0.061
$A^{0,\,\rm e}_{\rm FB}$	0.0157±0.0028
$A^{0,\,\mu}_{\rm FB}$	0.0163±0.0016
$A^{0,\,\tau}_{\rm FB}$	0.0206±0.0023

Table 4: Average line shape and asymmetry parameters from the data of the four LEP experiments given in Table 3, without the assumption of lepton universality. The χ^2/d.o.f. of the average is 36/27.

	$m_{\rm Z}$	$\Gamma_{\rm Z}$	$\sigma^0_{\rm h}$	$R_{\rm e}$	R_μ	R_τ	$A^{0,\,\rm e}_{\rm FB}$	$A^{0,\,\mu}_{\rm FB}$	$A^{0,\,\tau}_{\rm FB}$
$m_{\rm Z}$	1.00	−0.08	0.02	0.03	−0.02	−0.01	0.02	0.07	0.04
$\Gamma_{\rm Z}$	−0.08	1.00	−0.12	−0.01	0.00	0.00	0.00	0.00	0.00
$\sigma^0_{\rm h}$	0.02	−0.12	1.00	0.08	0.12	0.08	0.01	0.00	0.00
$R_{\rm e}$	0.03	−0.01	0.08	1.00	0.08	0.03	−0.06	0.01	0.01
R_μ	−0.02	0.00	0.12	0.08	1.00	0.06	0.00	0.01	0.00
R_τ	−0.01	0.00	0.08	0.03	0.06	1.00	0.00	0.00	0.01
$A^{0,\,\rm e}_{\rm FB}$	0.02	0.00	0.01	−0.06	0.00	0.00	1.00	−0.04	−0.02
$A^{0,\,\mu}_{\rm FB}$	0.07	0.00	0.00	0.01	0.01	0.00	−0.04	1.00	0.07
$A^{0,\,\tau}_{\rm FB}$	0.04	0.00	0.00	0.01	0.00	0.01	−0.02	0.07	1.00

Table 5: The correlation matrix for the set of parameters given in Table 4.

	ALEPH	DELPHI	L3	OPAL
$m_{\rm Z}$(GeV)	91.1924±0.0037	91.1849±0.0034	91.1938±0.0036	91.1846±0.0035
$\Gamma_{\rm Z}$(GeV)	2.4951±0.0056	2.4913±0.0054	2.5022±0.0054	2.4959±0.0053
$\sigma^0_{\rm h}$(nb)	41.56±0.09	41.40±0.10	41.48±0.11	41.47±0.10
R_ℓ	20.739±0.060	20.708±0.073	20.811±0.076	20.851±0.059
$A^{0,\ell}_{\rm FB}$	0.0195±0.0021	0.0182±0.0025	0.0186±0.0030	0.0142±0.0020
χ^2/d.o.f.	187/189	155/139	122/142	$15/10^{(a)}$

Table 6: Line shape and asymmetry parameters from 5-parameter fits to the data of the four LEP experiments, assuming lepton universality. R_ℓ is defined as $R_\ell \equiv \Gamma_{\rm had}/\Gamma_{\ell\ell}$, where $\Gamma_{\ell\ell}$ refers to the partial Z width for the decay into a pair of massless charged leptons.
$^{(a)}$This parameter set has been obtained by a parameter transformation applied to the 15 parameters of the OPAL fit.

Parameter	Average Value
$m_{\rm Z}$(GeV)	91.1884±0.0022
$\Gamma_{\rm Z}$(GeV)	2.4963±0.0032
$\sigma^0_{\rm h}$(nb)	41.488±0.078
R_ℓ	20.788±0.032
$A^{0,\ell}_{\rm FB}$	0.0172±0.0012

Table 7: Average line shape and asymmetry parameters from the results of the four LEP experiments given in Table 6, assuming lepton universality. R_ℓ is defined as $R_\ell \equiv \Gamma_{\rm had}/\Gamma_{\ell\ell}$, where $\Gamma_{\ell\ell}$ refers to the partial Z width for the decay into a pair of massless charged leptons. The χ^2/d.o.f. of the average is 39/31.

	$m_{\rm Z}$	$\Gamma_{\rm Z}$	$\sigma^0_{\rm h}$	R_ℓ	$A^{0,\ell}_{\rm FB}$
$m_{\rm Z}$	1.00	−0.08	0.02	0.00	0.08
$\Gamma_{\rm Z}$	−0.08	1.00	−0.12	−0.01	0.00
$\sigma^0_{\rm h}$	0.02	−0.12	1.00	0.15	0.01
R_ℓ	0.00	−0.01	0.15	1.00	0.00
$A^{0,\ell}_{\rm FB}$	0.08	0.00	0.01	0.00	1.00

Table 8: The correlation matrix for the set of parameters given in Table 7.

Without Lepton Universality:	
$\Gamma_{\rm ee}$ (MeV)	83.92±0.17
$\Gamma_{\mu\mu}$ (MeV)	83.92±0.23
$\Gamma_{\tau\tau}$ (MeV)	83.85±0.29

With Lepton Universality:	
$\Gamma_{\ell\ell}$ (MeV)	83.93±0.14
$\Gamma_{\rm had}$ (MeV)	1744.8±3.0
$\Gamma_{\rm inv}$ (MeV)	499.9±2.5

Table 9: Partial decay widths of the Z boson, derived from the results of the 9-parameter (Tables 4 and 5) and the 5-parameter fit (Tables 7 and 8). In the case of lepton universality, $\Gamma_{\ell\ell}$ refers to the partial Z width for the decay into a pair of massless charged leptons.

3 The τ Polarization

The τ polarization, $\mathcal{P}_\tau$, is determined by an indirect measurement of the longitudinal polarization of τ pairs produced in Z decays. It is defined as:

$$\mathcal{P}_\tau \equiv \frac{\sigma_R - \sigma_L}{\sigma_R + \sigma_L}, \tag{4}$$

where σ_R and σ_L are the τ-pair cross sections for the production of a right-handed and left-handed τ^-, respectively. The angular distribution of $\mathcal{P}_\tau$ as a function of the angle θ between the e^- and the τ^-, for $\sqrt{s} = m_Z$, is given by:

$$\mathcal{P}_\tau(\cos\theta) = -\frac{\mathcal{A}_\tau(1+\cos^2\theta) + 2\mathcal{A}_e\cos\theta}{1+\cos^2\theta + 2\mathcal{A}_\tau\mathcal{A}_e\cos\theta}, \tag{5}$$

with $\mathcal{A}_e$ and $\mathcal{A}_\tau$ as defined in Equation (3). Equation (5) neglects corrections for the effects of γ exchange, γZ interference and electromagnetic radiative corrections for initial- and final-state radiation. These effects are, however, taken into account in the experimental analyses. In particular, these corrections account for the $\sqrt{s}$ dependence of the tau polarization, $\mathcal{P}_\tau(\cos\theta)$, which is important since the off-peak data are included in the event samples for all experiments. When averaged over all production angles $\mathcal{P}_\tau$ is a measurement of $\mathcal{A}_\tau$. As a function of $\cos\theta$, $\mathcal{P}_\tau(\cos\theta)$ provides nearly independent determinations of both $\mathcal{A}_\tau$ and $\mathcal{A}_e$, thus allowing a test of the universality of the couplings of the Z to e and τ.

Each experiment makes separate $\mathcal{P}_\tau$ measurements using the five τ decay modes $e\nu\overline{\nu}$, $\mu\nu\overline{\nu}$, $\pi\nu$, $\rho\nu$ and $a_1\nu$ [29–32]. The $\rho\nu$ and $\pi\nu$ are the most sensitive channels, contributing weights of about 40% each in the average. In addition, DELPHI has used an inclusive hadronic analysis. The combination is made of the results from each experiment already averaged over the τ decay modes.

A discussion of the effects of possible common systematic errors between the experiments can be found in [1]. Further study of the uncertainties from the effects of radiative corrections for the ρ decay mode of the τ is desirable.

3.1 Results

Tables 10 and 11 show the most recent results for $\mathcal{A}_\tau$ and $\mathcal{A}_e$ obtained by the four experiments [29–32] and their combination. No common systematics are included in these averages. The statistical correlation between the extracted values of $\mathcal{A}_\tau$ and $\mathcal{A}_e$ is small ($\leq 5\%$), and is neglected.

The average values for $\mathcal{A}_\tau$ and $\mathcal{A}_e$:

$$\mathcal{A}_\tau = 0.1418 \pm 0.0075 \tag{6}$$
$$\mathcal{A}_e = 0.1390 \pm 0.0089, \tag{7}$$

are compatible, as is expected from lepton universality. Assuming $e - \tau$ universality, the values for $\mathcal{A}_\tau$ and $\mathcal{A}_e$ can be combined. This combination is performed neglecting any possible common systematic error between $\mathcal{A}_\tau$ and $\mathcal{A}_e$ within a given experiment. Such errors are estimated to be small, but warrant further study. The combined result of $\mathcal{A}_\tau$ and $\mathcal{A}_e$ gives:

$$\mathcal{A}_\ell = 0.1406 \pm 0.0057. \tag{8}$$

ALEPH	('90 - '92), final	$0.136 \pm 0.012 \pm 0.009$
DELPHI	('90 - '92), final	$0.148 \pm 0.017 \pm 0.014$
L3	('90 - '94), prel.	$0.152 \pm 0.010 \pm 0.009$
OPAL	('90 - '94), prel.	$0.134 \pm 0.010 \pm 0.009$
LEP Average		0.1418 ± 0.0075

Table 10: LEP results for $\mathcal{A}_\tau$. The χ^2/d.o.f. for the average is 1.1/3. The first error is statistical and the second systematic. In the LEP average, statistical and systematic error are combined in quadrature. The systematic component of the error, obtained by combining the individual systematic errors, is ± 0.0049.

ALEPH	('90 - '92), final	$0.129 \pm 0.016 \pm 0.005$
DELPHI	('90 - '92), final	$0.136 \pm 0.027 \pm 0.003$
L3	('90 - '94), prel.	$0.156 \pm 0.016 \pm 0.005$
OPAL	('90 - '94), prel.	$0.134 \pm 0.015 \pm 0.004$
LEP Average		0.1390 ± 0.0089

Table 11: LEP results for $\mathcal{A}_e$. The χ^2/d.o.f. for the average is 1.5/3. The first error is statistical and the second systematic. In the LEP average, statistical and systematic error are combined in quadrature. The systematic component of the error, obtained by combining the individual systematic errors, is ± 0.0020.

4 Results from b and c Quarks

The relevant quantities measured in the heavy quark sector at LEP are:

- The ratios of the b and c quark partial widths of the Z to its total hadronic partial width: $R_{\mathrm{b}} \equiv \Gamma_{\mathrm{b\bar{b}}}/\Gamma_{\mathrm{had}}$ and $R_{\mathrm{c}} \equiv \Gamma_{\mathrm{c\bar{c}}}/\Gamma_{\mathrm{had}}$.
- The forward-backward asymmetries, $A_{\mathrm{FB}}^{\mathrm{b\bar{b}}}$ and $A_{\mathrm{FB}}^{\mathrm{c\bar{c}}}$.
- The semileptonic branching ratios, BR($\mathrm{b} \to \ell$) and BR($\mathrm{b} \to \mathrm{c} \to \bar{\ell}$), and the average $\mathrm{B}^0\overline{\mathrm{B}^0}$ mixing parameter, $\overline{\chi}$. These are often determined at the same time as the widths or asymmetries in multiparameter fits to lepton tag samples. They are included in the combination procedure to take into account their correlations with the other parameters measured in the same fit.

There are several motivations for the averaging procedure. Several analyses measure more than one parameter simultaneously, for example the lepton fits. Some of the measurements of electroweak parameters depend explicitly on the values of other parameters, for example R_{b} depends on R_{c}. The common tagging and analysis techniques lead to common sources of systematic uncertainty, in particular for the double-tag measurements of R_{b}. The starting point for the combination is to ensure that all the analyses use a common set of assumptions for input parameters which give rise to systematic uncertainties [33]. The correlations and interdependences of the input measurements are then taken into account in a χ^2 minimization which results in the combined electroweak parameters and their correlation matrix. The only significant correlation between any of the resulting electroweak parameters turns out to be between R_{b} and R_{c}. This is discussed at the end of this section.

In a first fit the asymmetry measurements on peak, above peak and below peak were combined at each centre-of-mass energy. The results of this fit are given in [34]. The dependence of the average asymmetries on centre-of-mass energy agrees with the prediction of the Standard Model. To derive the pole asymmetries, $A_{\mathrm{FB}}^{0,\mathrm{q}}$, from the quark asymmetries, all the off-peak asymmetry measurements were then corrected to the peak energy before combining. Only results from this second fit are quoted here. There are therefore 7 parameters in total to be determined in the combination procedure: the two partial widths, two asymmetries, two semileptonic branching ratios and the average mixing parameter.

Recently the SLD collaboration has presented precise measurements of R_{b} [13] and of the left-right forward-backward asymmetry for b and c quarks [12]. Since the precision and the dominant sources of systematic uncertainty are similar at LEP and SLD it is useful to produce combined LEP+SLD averages. The left-right forward-backward asymmetries are, in contrast to the unpolarized forward-backward asymmetries, only sensitive to the final state couplings ($\mathcal{A}_{\mathrm{b}}$ and $\mathcal{A}_{\mathrm{c}}$). They are treated in the averaging procedure as physically independent quantities. However the methods to measure the polarized and unpolarized asymmetries are very similar, so $\mathcal{A}_{\mathrm{b}}$ and $\mathcal{A}_{\mathrm{c}}$ are included in the averaging procedure in order to estimate the correlation between the SLD and the LEP asymmetries, resulting in a 9-parameter fit.

4.1 Summary of measurements and averaging procedure

The measurements of R_{b} and R_{c} fall into two categories. In the first, called a single-tag measurement, a method to select b or c events is devised, and the number of tagged events is counted. This number must then be corrected for backgrounds from other flavours and for the tagging efficiency to calculate

the true fraction of hadronic Z decays of that flavour. The dominant systematic errors come from understanding the branching ratios and detection efficiencies which give the overall tagging efficiency. For the second technique, called a double-tag measurement, the event is divided into two hemispheres. For an $R_{\rm b}$ measurement, writing the number of tagged single hemispheres as N_t, the number of events with both hemispheres tagged as N_{tt}, then for a total of $N_{\rm had}$ hadronic Z decays:

$$\begin{aligned} \frac{N_t}{2N_{\rm had}} &= \varepsilon^{\rm b} R_{\rm b} + \varepsilon^{\rm c} R_{\rm c} + \varepsilon^{\rm uds}(1 - R_{\rm b} - R_{\rm c}), \\ \frac{N_{tt}}{N_{\rm had}} &= \mathcal{C}_{\rm b}(\varepsilon^{\rm b})^2 R_{\rm b} + (\varepsilon^{\rm c})^2 R_{\rm c} + (\varepsilon^{\rm uds})^2(1 - R_{\rm b} - R_{\rm c}), \end{aligned}$$

where $\varepsilon^{\rm b}$, $\varepsilon^{\rm c}$ and $\varepsilon^{\rm uds}$ are the tagging efficiencies per hemisphere for b, c and light-quark events, and $\mathcal{C}_{\rm b} \neq 1$ accounts for the fact that the tagging efficiencies between the hemispheres may be correlated. In practice, $\varepsilon^{\rm b} \gg \varepsilon^{\rm c} \gg \varepsilon^{\rm uds}$, $\mathcal{C}_{\rm b} \approx 1$, and the correlations for the other flavours are neglected. These equations can be solved to give $R_{\rm b}$ and $\varepsilon^{\rm b}$, which neglecting the c and uds backgrounds and the correlations are approximately given by:

$$\begin{aligned} \varepsilon^{\rm b} &\approx 2N_{tt}/N_t, \\ R_{\rm b} &\approx N_t^2/(4N_{tt}N_{\rm had}). \end{aligned}$$

The double-tagging method has the advantage that the tagging efficiency is derived directly from the data, reducing the systematic error of the measurement. The residual background of other flavours in the sample, and the evaluation of the correlation between the tagging efficiencies in the two hemispheres of the event are the main sources of systematic uncertainty in such an analysis.

The measurements included are [35]:

- Lepton fits from all four LEP experiments [36–40]. Each fit measures several parameters chosen from: $R_{\rm b}$, $R_{\rm c}$, $A_{\rm FB}^{\rm b\bar{b}}$, $A_{\rm FB}^{\rm c\bar{c}}$, BR(b $\to \ell$) and BR(b $\to$ c $\to \bar{\ell}$), and $\overline{\chi}$. The measured parameters are correlated. These analyses use hadronic events with one or more leptons in the final state. The semileptonic branching ratios can therefore be measured by a double-tagging technique if the lepton identification efficiency is known. The dominant sources of systematic error for the lepton fits arise from the lepton identification, from other semileptonic branching ratios and from the modelling of the semileptonic decay.

- Event-shape tag for $R_{\rm b}$ from ALEPH (double tag) and L3 (single tag) [41, 42].

- Lifetime (and lepton) double tag measurements for $R_{\rm b}$ from ALEPH, DELPHI, OPAL and SLD [13, 43–45]. These are the most precise determinations of $R_{\rm b}$, and dominate the combined result. The features of the double-tag technique were discussed above. These results depend explicitly on the assumed value of $R_{\rm c}$.

- Measurements of $A_{\rm FB}^{\rm b\bar{b}}$ based on lifetime tagged events with a hemisphere charge measurement from ALEPH , DELPHI and OPAL where the mean b-hemisphere charge is derived from the charge distributions themselves [38, 46, 47]. These contribute roughly the same weight to the combined result as the lepton fits.

- Analyses with $\rm D/D^{*\pm}$ mesons to measure $R_{\rm c}$ from DELPHI and OPAL [48, 49], including for the first time double-tag measurements. Of the two DELPHI measurements of $R_{\rm c}$, the first is a single-tag measurement, using branching ratios determined at lower-energy machines and counting the number of $\rm D^0$, $\rm D^+$ and $\rm D^{*+}$ mesons (91-93 data). The second is a double-tag measurement using a slow pion tag in one or two hemispheres (91-94 data), which reduces the dependence on branching ratio measurements performed at lower-energy machines. There are

three OPAL measurements. The first is a single-tag measurement using D^* mesons, the second a double-tag measurement using a fully reconstructed D^* in one hemisphere and a slow-pion tag in the opposite hemisphere, which effectively gives a measurement of the branching ratio BR($c \rightarrow D^*$). The third makes the assumption that the production rates of D^0, D^+, D_s and Λ_c saturate the fragmentation of $c\bar{c}$, since every charm quark ends up in a ground state hadron before the weak decay. This is a single tag measurement, but is insensitive to uncertainties in the charm hadronisation, relying only on the decay branching ratios of the charm hadrons.

All of these R_c analyses typically use other event properties to separate on a statistical basis the charm hadrons coming from $b\bar{b}$ and $c\bar{c}$ events. The overall normalization of the $b\bar{b}$ contribution is therefore fixed by the data. It depends on the properties of $b\bar{b}$ events, but not on an assumed value of R_b.

- Analyses with a $D^{*\pm}$ meson to measure $A_{FB}^{c\bar{c}}$ and $A_{FB}^{b\bar{b}}$ from ALEPH, DELPHI and OPAL [38, 50, 51].

- Measurements of $\mathcal{A}_b$ and $\mathcal{A}_c$ from SLD [12]. These results use lepton, kaon, $D^{*\pm}$ and lifetime plus hemisphere charge tags, with similar sources of systematic error as the LEP asymmetry measurements.

These measurements are presented by the LEP and SLD collaborations in a consistent manner for the purpose of combination [33,35,52–54]. The tables prepared by the experiments include a detailed breakdown of the systematic error of each measurement and its dependence on other electroweak parameters. Where necessary, the experiments apply small corrections to their results in order to use agreed values and ranges for the input parameters used to calculate systematic errors. The measurements, corrected where necessary, are summarized in the Appendix in Tables 24-33, where the statistical and systematic errors are quoted separately. The correlated systematic entries are from sources shared with one or more other results in the table and are derived from the full breakdown of common systematic uncertainties. The uncorrelated systematic entries are from the remaining sources.

The χ^2 minimization procedure used to derive the values of the heavy-flavour electroweak parameters was already used last year [1, 35, 53, 54]. The explicit dependences of each measurement on the other parameters is taken into account, for example the dependence of the value of R_b on the assumed value of R_c as described below. The full statistical and systematic covariance matrix for all the measurements is calculated. The correlation matrices relating several measurements made in the same analyses are used, in particular for the multiparameter lepton fits. Additional correlations arising from common sources of systematic uncertainty are estimated from a detailed breakdown of systematic errors [35]. For the common systematic errors, this breakdown for the double-tag measurements of R_b, plus the L3 event-shape analysis which also measures this single parameter, is given for illustration in Table 12. Similarly, a list of the correlated systematic errors for measurements of R_c relying on D and $D^{*\pm}$ mesons is given in Table 13.

Since c-quark events form the main background in the R_b analyses, the value of R_b depends on the value of R_c. If R_b and R_c are measured in the same analysis, this is reflected in the correlation matrix for the results. Otherwise the normalization of the charm contribution is not fixed by the data, and the measurement of R_b depends on the assumed value of R_c, which may be written as:

$$R_b = R_b^{meas} + a(R_c)\frac{(R_c - R_c^{used})}{R_c}. \qquad (9)$$

In this expression, R_b^{meas} is the result of the analysis assuming a value of $R_c = R_c^{used}$. The values of R_c^{used} and the coefficients $a(R_c)$ are given in Table 24 where appropriate. The dependences of all

	ALEPH shape [41]	ALEPH lifetime [43]	DELPHI multiple [44]	L3 shape [42]	OPAL multiple [45]	SLD lifetime [13]
Charm production	0.0	−0.85	−1.0	0.0	−0.94	−1.25
D^0 lifetime	0.0	−0.28	−0.2	0.0	−0.23	−0.24
D^+ lifetime	0.0	−0.36	−0.2	0.0	−0.29	−0.15
D_s lifetime	0.0	−0.22	−0.2	0.0	−0.17	−0.17
D decay multiplicity	0.0	−0.57	−0.4	0.0	−0.76	−1.80
BR(D→K^0)	0.0	0.0	+0.6	0.0	+0.59	0.0
Gluon splitting: $g \to b\bar{b}, c\bar{c}$	0.0	−0.33	−0.2	0.0	−0.46	−0.40
Long-lived light hadrons	0.0	−0.24	−0.4	0.0	−0.33	−0.09
BR($c \to \ell$)	+0.6	0.0	−0.2	0.0	−0.28	0.0
Semileptonic model $c \to \ell$	−2.1	0.0	−0.2	0.0	−0.25	0.0
$\langle x_E(c) \rangle$	+0.8	−0.12	−0.4	+1.8	−0.75	−1.22
Semileptonic model $b \to \ell$	−1.3	0.0	+0.2	0.0	0.0	0.0
$\langle x_E(b) \rangle$	0.0	0.0	0.0	−3.1	0.0	0.0
Total	2.7	1.2	1.5	3.6	1.7	2.6

Table 12: Example of breakdown of the correlated systematic error for R_b from lifetime, multiple and shape double-tag measurements (in units of 10^{-3}). The sign indicates the correlation of the measurement with the parameter describing the source of the error.

	DELPHI D inclusive [48]	DELPHI D exclusive [48]	OPAL $D^{*\pm}$ [49]	OPAL D^0, D^+, D_s, Λ_c [49]
$\langle x_E(c) \rangle$	0.000	0.000	0.001	0.007
$\langle x_E(b) \rangle$	−0.005	−0.002	0.000	−0.003
Average mixing	0.000	0.000	0.001	0.000
Gluon splitting: $g \to c\bar{c}$	0.000	0.000	0.003	0.002
BR($c \to D^* \to K\pi\pi_s$)	0.000	−0.015	−0.006	−0.000
B lifetime	0.004	0.004	0.001	0.005
D decay multiplicity and lifetime	0.000	0.000	0.001	0.001
D decay branching ratios	0.000	0.000	0.002	0.005
Total	0.006	0.017	0.007	0.010

Table 13: Breakdown of the correlated systematic errors for R_c from D and $D^{*\pm}$ related measurements. The inclusive DELPHI measurements is a double-tag method. The OPAL measurement denoted as $D^{*\pm}$ is a combination of the single tag $D^{*\pm}$ based analysis, and the measurement of BR($c \to D^* \to K\pi\pi_s$) using a double tag.

other measurements on other electroweak parameters are treated in the same way, with coefficients $a(x)$ describing the dependence on parameter x.

The results for BR($b \to \ell$) and BR($b \to c \to \bar{\ell}$) are now considered to be more reliable than those presented in the summer of 1994 [1]. This is because a sign error in the correlation coefficient of the uncertainty in the semileptonic decay model has been corrected [39], and the complete dependences of all the measurements on $\overline{\chi}$, BR($b \to \ell$) and BR($b \to c \to \bar{\ell}$) are now taken into account in the same way as their dependence on the other electroweak parameters.

4.2 Treatment of the LEP Asymmetry Measurements

For the 7-parameter fit described above, the peak and off-peak asymmetries were corrected to $\sqrt{s} = 91.26$ GeV, using the predicted dependence from ZFITTER [55]. The slope of the asymmetry around m_Z depends only on the axial coupling and the charge of the initial and final state fermions and is thus independent of the value of the asymmetry itself.

After calculating the overall averages, the quark pole asymmetries, $A_{FB}^{0,q}$, were derived by applying the corrections described below. The input measured asymmetries are all corrected to full acceptance and use the thrust axis as an estimate of the quark direction before gluon radiation. To relate the pole asymmetries to these numbers a few corrections that are summarized in Table 14 have to be applied:

- Energy shift to $\sqrt{s} = m_Z$ and QED corrections: The corrections due to the energy shift and initial state radiation have been calculated using ZFITTER [55].

- QCD corrections: The QCD corrections, using the thrust axis to define θ for the event, have been calculated to first order, including mass corrections [56]. The correction is given by $A_{FB}^{QCD} = A_{FB}^{no\,QCD}(1 + c\frac{\alpha_s}{\pi})$, with $c = -0.87$ for charm and $c = -0.79$ for bottom quarks. Assuming $\alpha_s(m_Z^2) = 0.12$ and varying the renormalization scale between $\mu^2 = (m_Z/4)^2$ and $\mu^2 = m_Z^2$ the correction factor is 0.966 ± 0.004 for b quarks, and 0.963 ± 0.004 for c quarks. There is an additional uncertainty in the QCD correction coming from whether the experimental event selection requirements bias the relative rates of 2- and 3-jet events in the sample. The error on the correction factor has therefore been increased to 0.010 for both b and c quarks. The resulting additive corrections to the asymmetries due to QCD corrections are provided in Table 14.

- γ exchange, γZ interference: These very small corrections have again been calculated using ZFITTER.

The lifetime/jet-charge measurements of asymmetries take into account QCD effects as an inherent part of the analysis, but the measured asymmetries for the analyses using a lepton or D^* tag need to be corrected for the effects of QCD on the event thrust axis direction. In order to perform a consistent average with the other asymmetry measurements, the jet-charge measurements were adjusted by subtracting 0.0033 from each of the three $A_{FB}^{b\bar{b}}(pk)$ jet-charge measurements before averaging.

Source	δA_{FB}^{b}	δA_{FB}^{c}
$\sqrt{s} = m_Z$	–0.0013	–0.0034
QED corrections	+0.0041	+0.0104
QCD corrections	$+0.0033 \pm 0.0010$	$+0.0023 \pm 0.0007$
γ, γZ	–0.0003	–0.0008
Total	$+0.0058 \pm 0.0010$	$+0.0085 \pm 0.0007$

Table 14: Corrections to be applied to the quark asymmetries. The corrections are to be understood as $A_{FB}^0 = A_{FB}^{meas} + \sum_i (\delta A_{FB})_i$

4.3 Results

4.3.1 Results of the 7-parameter fit to LEP data

Using the full averaging procedure gives the following combined results for the electroweak parameters:

$$\begin{aligned} R_{\mathrm{b}} &= 0.2216 \pm 0.0017 \\ R_{\mathrm{c}} &= 0.1546 \pm 0.0074 \\ \mathrm{BR}(\mathrm{b} \to \ell) &= (11.10 \pm 0.23)\% \\ \mathrm{BR}(\mathrm{b} \to \mathrm{c} \to \bar{\ell}) &= (7.78 \pm 0.37)\% \\ \overline{\chi} &= 0.1147 \pm 0.0062 \\ A_{\mathrm{FB}}^{\mathrm{b\bar{b}}}(\mathrm{pk}) &= 0.0941 \pm 0.0030 \\ A_{\mathrm{FB}}^{\mathrm{c\bar{c}}}(\mathrm{pk}) &= 0.0640 \pm 0.0058\,, \end{aligned} \tag{10}$$

with a χ^2/dof of $54/(68-7)$. The corresponding correlation matrix is given in Table 15. Note the correlation of -0.34 between R_{b} and R_{c}.

	R_{b}	R_{c}	BR(1)	BR(2)	$\overline{\chi}$	$A_{\mathrm{FB}}^{\mathrm{b\bar{b}}}(\mathrm{pk})$	$A_{\mathrm{FB}}^{\mathrm{c\bar{c}}}(\mathrm{pk})$
R_{b}	1.00	–0.34	–0.11	–0.05	0.02	0.00	0.06
R_{c}	–0.34	1.00	0.02	0.16	–0.02	0.09	–0.07
BR(1)	–0.11	0.02	1.00	–0.26	0.19	–0.02	0.08
BR(2)	–0.05	0.16	–0.26	1.00	–0.31	–0.07	–0.17
$\overline{\chi}$	0.02	–0.02	0.19	–0.31	1.00	0.33	–0.00
$A_{\mathrm{FB}}^{\mathrm{b\bar{b}}}(\mathrm{pk})$	0.00	0.09	–0.02	–0.07	0.33	1.00	0.10
$A_{\mathrm{FB}}^{\mathrm{c\bar{c}}}(\mathrm{pk})$	0.06	–0.07	0.08	–0.17	–0.00	0.10	1.00

Table 15: The correlation matrix for the set of the 7 heavy flavour parameters given in Equation 10. BR(1) and BR(2) denote $\mathrm{BR}(\mathrm{b} \to \ell)$ and $\mathrm{BR}(\mathrm{b} \to \mathrm{c} \to \bar{\ell})$ respectively.

The correction to R_{b} (R_{c}) due to photon exchange is given by $+0.0003$ (-0.0003) [55]. The total corrections for the on-peak asymmetries to give the pole asymmetries are $+0.0058 \pm 0.0010$ and $+0.0085 \pm 0.0007$ for b and c respectively, as listed in Table 14. The results to be used in electroweak fits are then:

$$\begin{aligned} R_{\mathrm{b}} &= 0.2219 \pm 0.0017 \\ R_{\mathrm{c}} &= 0.1543 \pm 0.0074 \\ A_{\mathrm{FB}}^{0,\,\mathrm{b}} &= 0.0999 \pm 0.0031 \\ A_{\mathrm{FB}}^{0,\,\mathrm{c}} &= 0.0725 \pm 0.0058\,. \end{aligned} \tag{11}$$

If R_{c} is fixed to its Standard-Model prediction of 0.172, then the value of R_{b} is:

$$R_{\mathrm{b}}(R_{\mathrm{c}} = 0.172) = 0.2205 \pm 0.0016\,.$$

4.3.2 Results of the 9-parameter fit to LEP and SLD data

Including the SLD results on R_b, $\mathcal{A}_b$ and $\mathcal{A}_c$ into the fit the following results are obtained:

$$\begin{aligned} R_b &= 0.2216 \pm 0.0017 \\ R_c &= 0.1543 \pm 0.0074 \\ \mathrm{BR}(b \to \ell) &= (11.12 \pm 0.23)\% \\ \mathrm{BR}(b \to c \to \bar{\ell}) &= (7.76 \pm 0.36)\% \\ \overline{\chi} &= 0.1145 \pm 0.0061 \\ A_{FB}^{b\bar{b}}(\mathrm{pk}) &= 0.0939 \pm 0.0030 \\ A_{FB}^{c\bar{c}}(\mathrm{pk}) &= 0.0644 \pm 0.0058 \\ \mathcal{A}_b &= 0.841 \pm 0.053 \\ \mathcal{A}_c &= 0.606 \pm 0.090\,, \end{aligned} \tag{12}$$

with a χ^2/dof of $55/(74-9)$. The corresponding correlation matrix is given in Table 16. In deriving these results the parameters $\mathcal{A}_b$ and $\mathcal{A}_c$ have been treated as independent of the forward-backward asymmetries $A_{FB}^{b\bar{b}}(\mathrm{pk})$ and $A_{FB}^{c\bar{c}}(\mathrm{pk})$. The fit results of $\mathcal{A}_b$ and $\mathcal{A}_c$ take into account the LEP and SLD average values of R_b and R_c, whereas the input numbers assumed the Standard Model values. This accounts for the fit results being lower than the input measurements.

	R_b	R_c	BR(1)	BR(2)	$\overline{\chi}$	$A_{FB}^{b\bar{b}}(\mathrm{pk})$	$A_{FB}^{c\bar{c}}(\mathrm{pk})$	$\mathcal{A}_b$	$\mathcal{A}_c$
R_b	1.00	–0.35	–0.12	–0.05	0.02	0.01	0.06	–0.07	0.05
R_c	–0.35	1.00	0.02	0.15	–0.01	0.08	–0.06	0.07	–0.06
BR(1)	–0.12	0.02	1.00	–0.26	0.19	–0.02	0.07	–0.00	0.06
BR(2)	–0.05	0.15	–0.26	1.00	–0.30	–0.07	–0.17	–0.07	–0.10
$\overline{\chi}$	0.02	–0.01	0.19	–0.30	1.00	0.32	–0.00	0.12	0.02
$A_{FB}^{b\bar{b}}(\mathrm{pk})$	0.01	0.08	–0.02	–0.07	0.32	1.00	0.11	0.06	–0.03
$A_{FB}^{c\bar{c}}(\mathrm{pk})$	0.06	–0.06	0.07	–0.17	–0.00	0.11	1.00	–0.02	0.07
$\mathcal{A}_b$	–0.07	0.07	–0.00	–0.07	0.12	0.06	–0.02	1.00	0.07
$\mathcal{A}_c$	0.05	–0.06	0.06	–0.10	0.02	–0.03	0.07	0.07	1.00

Table 16: The correlation matrix for the set of the 9 heavy flavour parameters given in Equation 12. BR(1) and BR(2) denote $\mathrm{BR}(b \to \ell)$ and $\mathrm{BR}(b \to c \to \bar{\ell})$ respectively.

The $\mathcal{A}_b$ and $\mathcal{A}_c$ values are already corrected for all QED and QCD effects. Correcting the partial widths for photon exchange, and the forward-backward asymmetries to give the pole asymmetries, yields:

$$\begin{aligned} R_b &= 0.2219 \pm 0.0017 \\ R_c &= 0.1540 \pm 0.0074 \\ A_{FB}^{0,\,b} &= 0.0997 \pm 0.0031 \\ A_{FB}^{0,\,c} &= 0.0729 \pm 0.0058 \\ \mathcal{A}_b &= 0.841 \pm 0.053 \\ \mathcal{A}_c &= 0.606 \pm 0.090\,. \end{aligned} \tag{13}$$

If R_c is fixed to its Standard-Model prediction of 0.172, then the value of R_b is:

$$R_b(R_c = 0.172) = 0.2205 \pm 0.0016\,.$$

It is not yet clear to what extent the uncertainty in the QCD correction is correlated between the LEP and SLD results. The possible correlation has been neglected here. If one assumes this error to be fully correlated the correlation between $A_{\rm FB}^{0,\,\rm b}$ and $\mathcal{A}_{\rm b}$ would increase by 0.04 and the one between $A_{\rm FB}^{0,\,\rm c}$ and $\mathcal{A}_{\rm c}$ would increase by 0.01. All other elements of the correlation matrix remain unchanged.

4.4 Comments on the correlation between $R_{\rm b}$ and $R_{\rm c}$

As noted before, the only large correlation between any of the combined electroweak parameters in Equations 11 and 13 is between $R_{\rm b}$ and $R_{\rm c}$. It is useful to examine how the correlations and interdependencies of the input measurements lead to this correlation between the combined parameters.

The measurements of $R_{\rm c}$ are almost independent of an assumed value for $R_{\rm b}$. For the lepton fit analyses, there is a very small net correlation between the two partial widths. There is a negative statistical correlation from events moving between the b and c contributions to the lepton sample. The overall systematic correlation is positive, dominated by effects such as the subtraction of hadronic background to the lepton sample, or the lepton identification efficiency which affect the b and c contributions in the same way. The net correlation from statistical and systematic effects is small.

The D and $\rm D^*$ meson measurements of $R_{\rm c}$ are constructed to be independent of an assumed value for $R_{\rm b}$, because they make a statistical separation of the b and c contributions based on other event properties. The overall normalization of the b contribution is therefore fixed by the data. These results depend on the features of b-hadron decay, but not on an assumed value of $R_{\rm b}$.

The precise double-tag measurements of $R_{\rm b}$ dominate the combined $R_{\rm b}$ result. The value of $R_{\rm b}$ from these measurements depend explicitly on the value of $R_{\rm c}$ assumed, and this dependence combined with the current error on $R_{\rm c}$ is almost entirely responsible for the size of the correlation coefficient between $R_{\rm b}$ and $R_{\rm c}$.

5 The Hadronic Charge Asymmetry $\langle Q_{FB} \rangle$

The LEP experiments ALEPH [57–59], DELPHI [60], and OPAL [61,62] have provided measurements of the hadronic charge asymmetry based on the mean difference in jet charges measured in the forward and backward event hemispheres, $\langle Q_{FB} \rangle$. DELPHI has also provided a related measurement of the total charge asymmetry by making a charge assignment on an event-by-event basis and performing a likelihood fit. The experimental values quoted for the average forward-backward charge difference $\langle Q_{FB} \rangle$, cannot be directly compared as some of them include detector dependent effects such as acceptances and efficiencies. We therefore use the effective electroweak mixing angle, $\sin^2\theta^{lept}_{eff}$, defined in Section 6.3, as a means of combining the experimental results summarized in Table 17.

Experiment		$\sin^2\theta^{lept}_{eff}$
ALEPH	90-93, prel.	$0.2323 \pm 0.0010 \pm 0.0010$
DELPHI	90-91, final	$0.2345 \pm 0.0030 \pm 0.0027$
OPAL	91-94, prel.	$0.2326 \pm 0.0012 \pm 0.0013$
Average		0.2325 ± 0.0013

Table 17: Summary of the determination of $\sin^2\theta^{lept}_{eff}$ from inclusive hadronic charge asymmetries at LEP. For each experiment, the first error is statistical and the second systematic. The latter is dominated by fragmentation and decay modelling uncertainties.

The dominant source of systematic error arises from the modelling of the charge flow in the fragmentation process for each flavour. Both ALEPH and OPAL measure the required charge properties for $Z \to b\bar{b}$ events from the data. ALEPH has also determined the charm charge properties from the data. The fragmentation model implemented in the JETSET Monte-Carlo program [63] is used by all experiments as reference; the one of the HERWIG Monte-Carlo program [64] is used for comparison. The JETSET fragmentation parameters are varied to estimate the systematic errors. The central values chosen by the experiments for these parameters are, however, not the same. The degree of correlation between the fragmentation uncertainties for the different experiments requires further investigation. We treat them as fully correlated. The present average of $\sin^2\theta^{lept}_{eff}$ from $\langle Q_{FB} \rangle$ is not very sensitive to the treatment of common uncertainties.

The ambiguities due to QCD corrections may cause changes in the derived value of $\sin^2\theta^{lept}_{eff}$, which are, however, well below the fragmentation uncertainties and experimental errors. The estimated systematic uncertainties from this source are considered fully correlated between experiments.

There is also some correlation between these results and those for $A^{b\bar{b}}_{FB}$ using jet charges. The dominant source of correlation is again through uncertainties in the fragmentation and decay models used. The typical correlation between the derived values of $\sin^2\theta^{lept}_{eff}$ between the $\langle Q_{FB} \rangle$ and the $A^{b\bar{b}}_{FB}$ jet charge measurement has been estimated to be between 20% and 25%. This leads to only a small change in the relative weights for the $A^{b\bar{b}}_{FB}$ and $\langle Q_{FB} \rangle$ results when averaging their $\sin^2\theta^{lept}_{eff}$ values (Section 6.3). Furthermore, the jet charge method contributes at most half of the weight of the $A^{b\bar{b}}_{FB}$ measurement. Thus, the correlation between $\langle Q_{FB} \rangle$ and $A^{b\bar{b}}_{FB}$ from jet charge will have little impact on the overall Standard Model fit, and is neglected at present.

6 Interpretation of Results

6.1 The Coupling Parameters $\mathcal{A}_f$

The coupling parameters $\mathcal{A}_f$ are defined in terms of the effective vector and axial-vector neutral current couplings of fermions (Equation (3)). The LEP measurements of the forward-backward asymmetries of charged leptons (Section 2) and b and c quarks (Section 4) determine the products $A_{FB}^{0,f} = \frac{3}{4}\mathcal{A}_e\mathcal{A}_f$ (Equation (2)). The LEP measurements of the τ polarization (Section 3), $\mathcal{P}_\tau(\cos\theta)$, determine $\mathcal{A}_\tau$ and $\mathcal{A}_e$ separately (Equation (5)). The SLD collaboration measures the left-right asymmetry, A_{LR} [10,11], which determines the same quantity, $\mathcal{A}_e$, as the τ polarization, with minimal model dependence. Both measurements have small systematic errors. The SLD measurements of the left-right forward-backward asymmetries for b and c quarks [12] are direct determinations of $\mathcal{A}_b$ and $\mathcal{A}_c$.

Table 18 shows the results on the leptonic coupling parameter $\mathcal{A}_\ell$ and their combination assuming lepton universality. Table 19 shows the results on the quark coupling parameters $\mathcal{A}_b$ and $\mathcal{A}_c$ derived from LEP measurements alone (Equation 11) and from the combination of LEP and SLD measurements (Equation 13).

	$\mathcal{A}_\ell$	Cumulative Average	χ^2/d.o.f.
$A_{FB}^{0,\ell}$	0.1514 ± 0.0053		
$\mathcal{P}_\tau(\cos\theta)$	0.1406 ± 0.0057	0.1464 ± 0.0039	1.9/1
A_{LR} (SLD)	0.1551 ± 0.0040	0.1506 ± 0.0028	4.4/2

Table 18: Comparison of the determinations of the leptonic coupling parameter $\mathcal{A}_\ell$ assuming lepton universality. The second column lists the $\mathcal{A}_\ell$ values derived from the quantities listed in the first column. The third column contains the cumulative averages of these $\mathcal{A}_\ell$ results. The averages are derived assuming no correlations between the measurements. The χ^2 per degree of freedom for the cumulative averages is given in the last column.

LEP	using $\mathcal{A}_\ell = 0.1464 \pm 0.0039$
$\mathcal{A}_b$	0.910 ± 0.037
$\mathcal{A}_c$	0.660 ± 0.056
LEP+SLD	**using $\mathcal{A}_\ell = 0.1506 \pm 0.0028$**
$\mathcal{A}_b$	0.871 ± 0.027
$\mathcal{A}_c$	0.635 ± 0.046

Table 19: Determinations of the quark coupling parameters $\mathcal{A}_b$ and $\mathcal{A}_c$ from LEP data alone (using the LEP average for $\mathcal{A}_\ell$) and from LEP+SLD data (using the LEP+SLD average for $\mathcal{A}_\ell$) assuming lepton universality.

6.2 The Effective Vector and Axial-Vector Coupling Constants

The partial widths of the Z into leptons and the lepton forward-backward asymmetries (Section 2), the τ polarization and the τ polarization asymmetry (Section 3) can be combined to determine the effective vector and axial-vector couplings for e, μ and τ. The asymmetries (Equations (2) and (5)) determine the ratio $g_{V\ell}/g_{A\ell}$ (Equation (3)), while the sum of the squares of the couplings is derived from the leptonic partial widths:

$$\Gamma_{\ell\ell} = \frac{G_{\rm F} m_{\rm Z}^3}{6\pi\sqrt{2}}(g_{V\ell}^2 + g_{A\ell}^2)(1+\delta_\ell^{QED}), \tag{14}$$

where $\delta_\ell^{QED} = 3q_\ell^2\alpha(m_{\rm Z}^2)/(4\pi)$ accounts for final state photonic corrections. Corrections due to lepton masses, neglected in Equation 14, are taken into account for the results presented below.

The averaged results for the effective lepton couplings are given in Table 20. Figure 2 shows the 68% probability contours in the $g_{A\ell}$-$g_{V\ell}$ plane. The signs of $g_{A\ell}$ and $g_{V\ell}$ are based on the convention $g_{A\rm e} < 0$. With this convention the signs of the couplings of all charged leptons follow from LEP data alone. For comparison, the $g_{V\ell}$-$g_{A\ell}$ relation following from the measurement of $A_{\rm LR}$ from SLD [10,11] is indicated as a band in the $g_{A\ell}$-$g_{V\ell}$-plane of Figure 2. It is consistent with the LEP data. The information on the leptonic couplings from LEP can therefore be combined with the $A_{\rm LR}$ measurement of SLD. The results for this combination are given in the right column of Table 20. The measured ratios of the e, μ and τ couplings provide a test of lepton universality and are also given in Table 20.

	Without Lepton Universality:	
	LEP	LEP+SLD
$g_{V\rm e}$	-0.0368 ± 0.0017	-0.03850 ± 0.00087
$g_{V\mu}$	-0.0370 ± 0.0041	-0.0354 ± 0.0036
$g_{V\tau}$	-0.0371 ± 0.0018	-0.0369 ± 0.0018
$g_{A\rm e}$	-0.50115 ± 0.00052	-0.50103 ± 0.00051
$g_{A\mu}$	-0.50113 ± 0.00076	-0.50124 ± 0.00075
$g_{A\tau}$	-0.50151 ± 0.00089	-0.50152 ± 0.00089
	Ratios of couplings:	
	LEP	LEP+SLD
$g_{V\mu}/g_{V\rm e}$	1.01 ± 0.14	0.92 ± 0.10
$g_{V\tau}/g_{V\rm e}$	1.008 ± 0.071	0.959 ± 0.052
$g_{A\mu}/g_{A\rm e}$	1.0000 ± 0.0018	1.0004 ± 0.0018
$g_{A\tau}/g_{A\rm e}$	1.0007 ± 0.0020	1.0010 ± 0.0020
	With Lepton Universality:	
	LEP	LEP+SLD
$g_{V\ell}$	-0.0369 ± 0.0010	-0.03797 ± 0.00071
$g_{A\ell}$	-0.50119 ± 0.00041	-0.50111 ± 0.00041
g_ν	$+0.5011 \pm 0.0013$	$+0.5011 \pm 0.0013$

Table 20: Results for the effective vector and axial-vector couplings derived from the combined LEP data without and with the assumption of lepton universality. For the right column the SLD measurement of $A_{\rm LR}$ is also included.

The neutrino couplings to the Z can be derived from the measured value of its invisible width, $\Gamma_{\rm inv}$, attributing it exclusively to the decay into three identical neutrino generations ($\Gamma_{\rm inv} = 3\Gamma_{\nu\nu}$) and assuming $g_{A\nu} \equiv g_{V\nu} \equiv g_\nu$. The relative sign of g_ν is chosen to be in agreement with neutrino scattering data [65], resulting in $g_\nu = +0.5011 \pm 0.0013$.

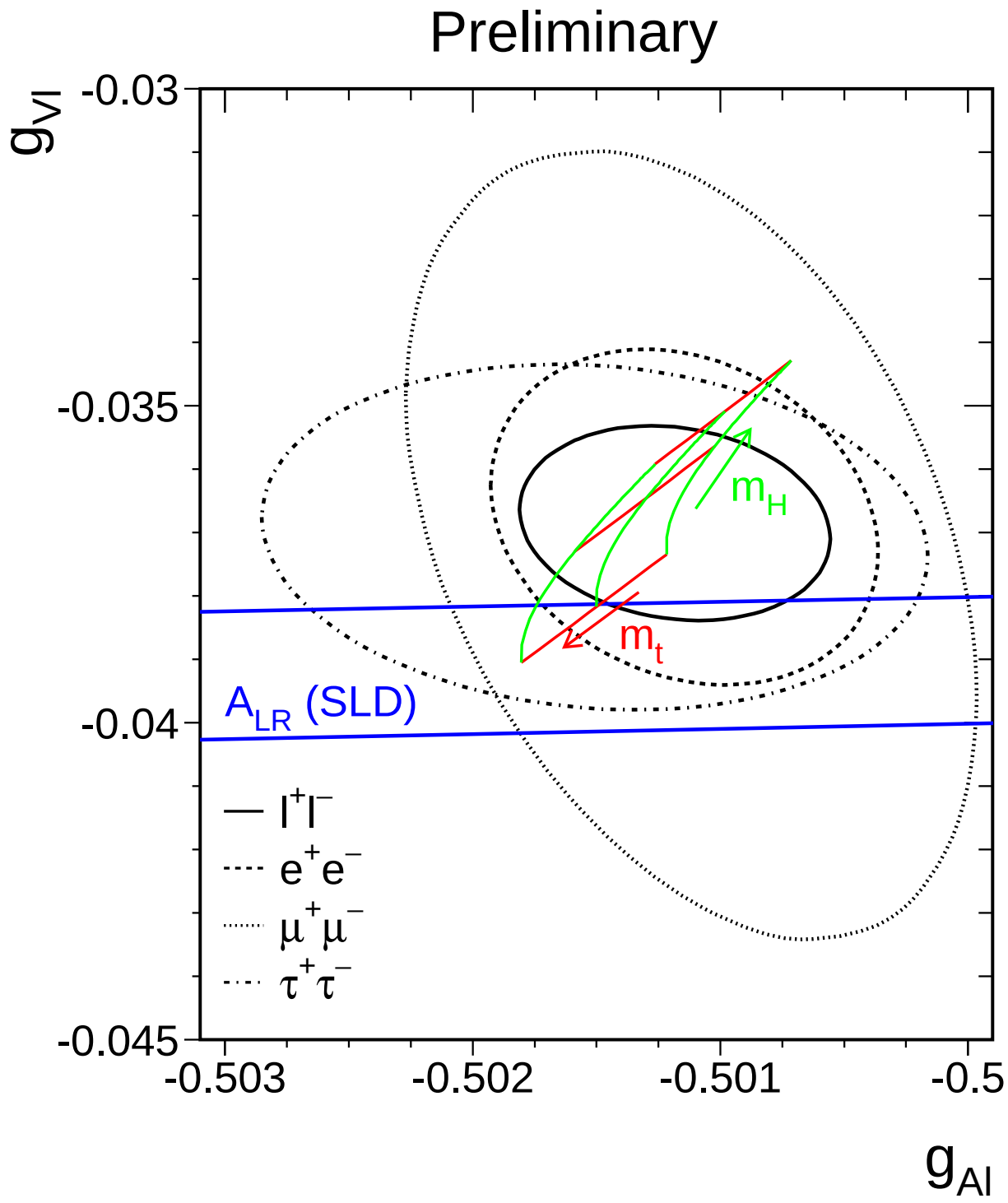

Figure 2: Contours of 68% probability in the $g_{V\ell}$-$g_{A\ell}$ plane from LEP measurements. The solid contour results from a fit assuming lepton universality. Also shown is the one standard deviation band resulting from the $A_{\rm LR}$ measurement of SLD. The grid corresponds to the Standard Model prediction for $m_{\rm t} = 180 \pm 12$ GeV and $m_{\rm H} = 300^{+700}_{-240}$ GeV. The arrows point in the direction of increasing values of $m_{\rm t}$ and $m_{\rm H}$.

6.3 The Effective Electroweak Mixing Angle $\sin^2\theta^{\rm lept}_{\rm eff}$

The asymmetry measurements from LEP can be combined into a single observable, the effective electroweak mixing angle, $\sin^2\theta^{\rm lept}_{\rm eff}$, defined as:

$$\sin^2\theta^{\rm lept}_{\rm eff} \equiv \frac{1}{4}(1 - g_{V\ell}/g_{A\ell})\,, \tag{15}$$

without making any strong model-specific assumptions.

For a combined average of $\sin^2\theta^{\rm lept}_{\rm eff}$ from $A^{0,\ell}_{\rm FB}$, $\mathcal{A}_\tau$ and $\mathcal{A}_{\rm e}$ only the assumption of lepton universality, already inherent in the definition of $\sin^2\theta^{\rm lept}_{\rm eff}$, is needed. In practice no further assumption is involved if the quark forward-backward asymmetries, $A^{\rm b\bar{b}}_{\rm FB}$ and $A^{\rm c\bar{c}}_{\rm FB}$, are included in this average, as these asymmetries have a reduced sensitivity to corrections particular to the hadronic vertex. The results of these determinations of $\sin^2\theta^{\rm lept}_{\rm eff}$ and their combination are shown in Table 21. Also the comparison with the measurement of the left-right asymmetry, $A_{\rm LR}$, from SLD [10,11] is given.

	$\sin^2\theta^{\rm lept}_{\rm eff}$	Average by Group of Observations	Cumulative Average	χ^2/d.o.f.
$A^{0,\ell}_{\rm FB}$	0.23096 ± 0.00068			
$\mathcal{A}_\tau$	0.23218 ± 0.00095			
$\mathcal{A}_{\rm e}$	0.2325 ± 0.0011	0.23160 ± 0.00049	0.23160 ± 0.00049	1.9/2
$A^{0,\rm b}_{\rm FB}$	0.23209 ± 0.00055			
$A^{0,\rm c}_{\rm FB}$	0.2318 ± 0.0013	0.23205 ± 0.00051	0.23182 ± 0.00035	2.4/4
$\langle Q_{\rm FB}\rangle$	0.2325 ± 0.0013	0.2325 ± 0.0013	0.23186 ± 0.00034	2.6/5
$A_{\rm LR}$ (SLD)	0.23049 ± 0.00050	0.23049 ± 0.00050	0.23143 ± 0.00028	7.8/6

Table 21: Comparison of several determinations of $\sin^2\theta^{\rm lept}_{\rm eff}$ from asymmetries. Averages are obtained as weighted averages assuming no correlations. The second column lists the $\sin^2\theta^{\rm lept}_{\rm eff}$ values derived from the quantities listed in the first column. The third column contains the averages of these numbers by groups of observations, where the groups are separated by the horizontal lines. The last column shows the cumulative averages. The χ^2 per degree of freedom for the cumulative averages is also given.

6.4 Number of Neutrino Species

An important aspect of our measurement concerns the information related to Z decays into invisible channels. Using the results of Tables 7 and 8, the ratio of the Z decay width into invisible particles and the leptonic decay width is determined:

$$\Gamma_{\rm inv}/\Gamma_{\ell\ell} \;=\; 5.956 \pm 0.031\,.$$

The Standard Model value for the ratio of the partial widths to neutrinos and charged leptons is:

$$(\Gamma_{\nu\nu}/\Gamma_{\ell\ell})_{\rm SM} \;=\; 1.991 \pm 0.001\,.$$

The central value is evaluated for $m_{\rm Z} = 91.1884$ GeV, $m_{\rm t} = 180$ GeV, $m_{\rm H} = 300$ GeV and the error quoted accounts for a variation of $m_{\rm t}$ in the range $m_{\rm t} = 180 \pm 12$ GeV and a variation of $m_{\rm H}$ in the range 60 GeV $\leq m_{\rm H} \leq$ 1000 GeV.

The number of light neutrino species is given by the ratio of the two expressions listed above:

$$N_\nu \quad = \quad 2.991 \pm 0.016\,.$$

6.5 Constraints on the Standard Model

The precise electroweak measurements performed at LEP can be used to check the validity of the Standard Model and, within its framework, to infer valuable information about its fundamental parameters. The accuracy of the measurements makes them sensitive to the top-quark mass, $m_{\rm t}$, and to the mass of the Higgs boson, $m_{\rm H}$, through loop corrections. The leading $m_{\rm t}$ dependence is quadratic and allows a determination of $m_{\rm t}$. The main dependence on $m_{\rm H}$ is logarithmic and therefore, with the present data accuracy, the constraints on $m_{\rm H}$ are still weak.

The various LEP measurements are summarized in Table 22a and are presented in Figures 3, 4 and 5, together with their Standard Model prediction as a function of $m_{\rm t}$. The bands in the Standard Model predictions reflect the linear sum of the expected variations in each quantity due to a change of the strong coupling constant $\alpha_s(m_{\rm Z}^2) = 0.123 \pm 0.006$ [66] and $m_{\rm H}$ in the interval 60 GeV $\leq m_{\rm H} \leq$ 1000 GeV for $m_{\rm Z} = 91.1884$ GeV.

Detailed studies of the theoretical uncertainties in the Standard Model predictions due to missing higher-order electroweak corrections and their interplay with QCD corrections are carried out in the working group on 'Precision calculations for the Z resonance' [67]. Theoretical uncertainties are evaluated by comparing different but, within our present knowledge, equivalent treatments of aspects such as resummation techniques, momentum transfer scales for vertex corrections and factorization schemes. The impact of these intrinsic theoretical uncertainties on $m_{\rm t}$ and $\alpha_s(m_{\rm Z}^2)$ has been estimated by repeating the Standard Model fits in this Section using several combinations of options which were implemented in the electroweak libraries used [68] for the study performed in [67]. As a result the maximal variations of the central values of the fitted parameters correspond to an additional theoretical error of less than 2 GeV on $m_{\rm t}$ and less than 0.001 on $\alpha_s(m_{\rm Z}^2)$. This error on $\alpha_s(m_{\rm Z}^2)$ covers missing higher-order electroweak corrections and uncertainties in the interplay of electroweak and QCD corrections but not the effect of missing higher-order QCD corrections. A discussion of theoretical uncertainties in the determination of α_s can be found in [67,69]. These theoretical errors have been neglected for the results presented in Table 23.

At present the impact of theoretical uncertainties on the determination of $m_{\rm t}$ from precise electroweak measurements is negligible compared to the error due to the uncertainty in the value of the fine structure constant $\alpha(m_{\rm Z}^2)$. The uncertainty in $\alpha(m_{\rm Z}^2)$ arises from the contribution of light quarks to the photon vacuum polarization. Recently there have been several reevaluations of $\alpha(m_{\rm Z}^2)$ [4–7]. For the results presented in this Section, a value of $\alpha(m_{\rm Z}^2) = 1/(128.896 \pm 0.090)$ [6] is used. This uncertainty causes an error of 0.00023 on the Standard Model prediction of $\sin^2\theta^{\rm lept}_{\rm eff}$ and an error of 4 GeV on $m_{\rm t}$, which are included in the results listed in Table 23. The effect on the Standard Model prediction for $\Gamma_{\ell\ell}$ is negligible. The $\alpha_s(m_{\rm Z}^2)$ values for the Standard Model fits presented in this Section are stable against a variation of $\alpha(m_{\rm Z}^2)$ in the interval quoted.

	Measurement with Total Error	Systematic Error	Standard Model	Pull
a) LEP				
line-shape and lepton asymmetries:				
m_Z [GeV]	91.1884 ± 0.0022	[a]0.0015	91.1882	0.1
Γ_Z [GeV]	2.4963 ± 0.0032	[a]0.0020	2.4973	−0.3
σ_h^0 [nb]	41.488 ± 0.078	0.077	41.450	0.5
R_ℓ	20.788 ± 0.032	0.026	20.773	0.5
$A_{FB}^{0,\ell}$	0.0172 ± 0.0012	0.0008	0.0159	1.1
+ correlation matrix Table 8				
τ polarization:				
$\mathcal{A}_\tau$	0.1418 ± 0.0075	0.0049	0.1455	−0.5
$\mathcal{A}_e$	0.1390 ± 0.0089	0.0020	0.1455	−0.7
b and c quark results:				
R_b [b]	0.2219 ± 0.0017	0.0014	0.2156	3.7
R_c [b]	0.1543 ± 0.0074	0.0063	0.1724	−2.5
$A_{FB}^{0,b}$ [b]	0.0999 ± 0.0031	0.0015	0.1020	−0.7
$A_{FB}^{0,c}$ [b]	0.0725 ± 0.0058	0.0029	0.0728	0.0
+ correlation matrix Table 15				
$q\bar{q}$ charge asymmetry:				
$\sin^2\theta_{eff}^{lept}$ ($\langle Q_{FB} \rangle$)	0.2325 ± 0.0013	0.0010	0.23172	0.6
b) SLD				
$\sin^2\theta_{eff}^{lept}$ (A_{LR} [10,11])	0.23049 ± 0.00050	0.00015	0.23172	−2.5
R_b [13][b]	0.2171 ± 0.0054	0.0037	0.2156	0.3
$\mathcal{A}_b$ [12]	0.841 ± 0.053	0.038	0.935	−1.8
$\mathcal{A}_c$ [12]	0.606 ± 0.090	0.048	0.667	−0.7
c) $p\bar{p}$ and νN				
m_W [GeV] ($p\bar{p}$ [70])	80.26 ± 0.16	0.13	80.35	−0.5
$1 - m_W^2/m_Z^2$ (νN [14–16])	0.2257 ± 0.0047	0.0043	0.2237	0.4

Table 22: Summary of measurements included in the combined analysis of Standard Model parameters. Section a) summarizes LEP averages, Section b) SLD results for $\sin^2\theta_{eff}^{lept}$ from the measurement of the left-right polarization asymmetry, for R_b and for $\mathcal{A}_b$ and $\mathcal{A}_c$ from polarized forward-backward asymmetries and Section c) electroweak precision measurements from $p\bar{p}$ colliders and νN scattering. The total errors given in column 2 include the systematic errors listed in column 3. The determination of the systematic part of each error is approximate. The Standard Model results in column 4 and the pulls (difference between measurement and fit in units of the total measurement error) in column 5 are derived from the Standard Model fit including all data (Table 23, column 4) for a fixed value of $m_H = 300$ GeV.

[a] The systematic errors on m_Z and Γ_Z contain the errors arising from the uncertainties in the LEP energy only.

[b] For fits which combine LEP and SLD heavy flavour measurements we use as input the heavy flavour results given in Equation (13) and their correlation matrix in Table 16 in Section 4 of this note.

	LEP	LEP + SLD	LEP + SLD + $p\bar{p}$ and νN data
m_t (GeV)	$170 \pm 10\ ^{+17}_{-19}$	$180\ ^{+8}_{-9}\ ^{+17}_{-20}$	$178 \pm 8\ ^{+17}_{-20}$
$\alpha_s(m_Z^2)$	$0.125 \pm 0.004 \pm 0.002$	$0.123 \pm 0.004 \pm 0.002$	$0.123 \pm 0.004 \pm 0.002$
χ^2/d.o.f.	18/9	28/12	28/14
$\sin^2\theta_{\rm eff}^{\rm lept}$	$0.23206 \pm 0.00028\ ^{+0.00008}_{-0.00017}$	$0.23166 \pm 0.00025\ ^{+0.00006}_{-0.00013}$	$0.23172 \pm 0.00024\ ^{+0.00007}_{-0.00014}$
$1 - m_W^2/m_Z^2$	$0.2247 \pm 0.0010\ ^{+0.0004}_{-0.0002}$	$0.2234 \pm 0.0009\ ^{+0.0005}_{-0.0002}$	$0.2237 \pm 0.0009\ ^{+0.0004}_{-0.0002}$
m_W (GeV)	$80.295 \pm 0.057\ ^{+0.011}_{-0.019}$	$80.359 \pm 0.051\ ^{+0.013}_{-0.024}$	$80.346 \pm 0.046\ ^{+0.012}_{-0.021}$

Table 23: Results of fits to LEP and other electroweak precision data for m_t and $\alpha_s(m_Z^2)$. No external constraint on $\alpha_s(m_Z^2)$ has been imposed. The second column presents the results obtained using LEP data only (Table 22a). The third column gives the result when the SLD measurements of the left-right asymmetry and electroweak heavy flavour results (Table 22b) are also added. In the fourth column also the combined data from $p\bar{p}$ colliders and νN experiments (Table 22c) are included. The central values and the first errors quoted refer to $m_H = 300$ GeV. The second errors correspond to the variation of the central value when varying m_H in the interval 60 GeV $\leq m_H \leq$ 1000 GeV. The bottom part of the table lists derived results for $\sin^2\theta_{\rm eff}^{\rm lept}$, $1 - m_W^2/m_Z^2$ and m_W.

Table 23 shows the constraints obtained on m_t and $\alpha_s(m_Z^2)$ when fitting the measurements in Table 22 to up-to-date Standard Model calculations [68]. The fits have been repeated for $m_H = 60$, 300 and 1000 GeV and the difference in the fitted parameters is quoted as the second uncertainty. The results obtained using only LEP data (Table 22a), as well as those obtained by including preliminary results from the SLD collaboration (Table 22b) for the left-right asymmetry, A_{LR} [10, 11], and the measurements with heavy flavours (R_b [13], $\mathcal{A}_b$ and $\mathcal{A}_c$ [12]) are shown in Table 23. The rightmost column of Table 23 gives the Standard Model constraints obtained by including in addition the published measurements of m_W from UA2 [17], CDF [18, 19], a preliminary result for m_W from DØ [20][3], and the measurements of the neutrino neutral to charged current ratios from CDHS [14], CHARM [15] and CCFR [16] (Table 22c).

The χ^2/d.o.f. values for all these fits have probabilities ranging from 0.6% to 3.5%. The measurements of R_b and R_c, dominated by systematic errors, cause a χ^2 contribution of approximately 15 for all the Standard Model fits in Table 23 (see also Table 22). In the Standard Model the predictions of R_b and R_c are not very sensitive to m_t and $\alpha_s(m_Z^2)$ compared to other input data of this analysis. If they are omitted from the fit the fitted value of m_t increases by only 4 GeV, and the value of $\alpha_s(m_Z^2)$ stays approximately constant.

The fitted value of m_t is in excellent agreement with the top mass values $m_t = 176 \pm 8$ (stat.) $\pm$ 10 (syst.) GeV and $m_t = 199^{+19}_{-21}$ (stat.) $\pm$ 22 (syst.) GeV reported from the observation of the top quark at the TEVATRON by the CDF [8] and the DØ collaborations [9], respectively. For the sake of comparison with electroweak precision data the weighted average of both measurements, $m_t = 180 \pm 12$ GeV, is used in this note.

As shown above, the fitted values of m_t are insensitive to whether or not R_b and R_c are included in the fits. This is to be expected as the constraint on m_t comes mainly from the leptonic sector. Figure 6 shows a comparison of the leptonic partial width from LEP (Table 9) and the effective electroweak

[3] See Reference 70 for a combination of these m_W measurements.

mixing angle from asymmetries measured at LEP and SLD (Table 21), with the Standard Model. Good agreement with the Standard Model prediction is observed. The star shows the prediction if, among the electroweak radiative corrections only the photon vacuum polarization is included, showing evidence that LEP/SLD data are sensitive to genuinely electroweak corrections.

The value of $\alpha_s(m_Z^2)$ derived from an analysis of electroweak precision tests within the Standard Model framework depends essentially on R_ℓ, Γ_Z and σ_h^0. The result is in very good agreement with that obtained from event-shape measurements at LEP ($\alpha_s(m_Z^2) = 0.123 \pm 0.006$ [66]) and of similar precision. The strong coupling constant can also be determined from the parameter R_ℓ alone. For $m_Z = 91.1884$ GeV, and imposing $m_t = 180 \pm 12$ GeV as a constraint, $\alpha_s = 0.126 \pm 0.005 \pm 0.002$ is obtained, where the second error accounts for the variation of the result when varying m_H in the range 60 GeV $\leq m_H \leq$ 1000 GeV.

The averages of R_b and R_c (Table 22) have a strong correlation (-0.35). If the value of R_c is fixed to the Standard Model value $R_c = 0.172$, ignoring the pull of R_c, the agreement between the R_b result and the Standard Model fit result improves from 3.7 to 3.2 standard deviations. In this case one obtains $R_b = 0.2205 \pm 0.0016$. If this deviation of R_b is attributed to the b partial width, then R_ℓ should also be affected since $\Gamma_{b\bar{b}}$ is a component of the total hadronic width [71]. In Figure 7 the fitted result for R_b with R_c fixed to its Standard Model value is plotted versus $\sin^2\theta_{eff}^{lept}$. If one assumes the Standard Model dependence of the partial widths on $\sin^2\theta_{eff}^{lept}$ for the light quarks and the c quark, and takes $\alpha_s(m_Z^2) = 0.123 \pm 0.006$, R_ℓ imposes a constraint on the two variables. The one-sigma R_ℓ band is centred on the Standard Model prediction while the R_b band is off-set. The overlap, however, depends on the value of $\alpha_s(m_Z^2)$; it improves if the value of $\alpha_s(m_Z^2)$ is reduced. As mentioned above, the fitted value of $\alpha_s(m_Z^2)$ is insensitive to whether or not R_b and R_c are included in the fit. However, its value could vary widely depending on the interpretation given to the deviation of R_b and R_c.

Figure 8 shows the χ^2 value for the Standard Model fits discussed in Table 23 column 4, as a function of m_t for the three values of m_H (60, 300 and 1000 GeV) considered. It can be seen that the minima of these curves occur at different values of χ^2. This suggests the possibility of extracting constraints on the value of m_H.

The main m_H dependence of the Standard Model predictions for the measurements listed in Table 22 is given by corrections proportional to $\log(m_H)$. The effects of m_H and m_t, however, are correlated for most observables, which weakens the determination of m_H without a direct measurement of m_t. Figure 9 shows the observed value of $\Delta\chi^2 \equiv \chi^2 - \chi^2_{min}$ as a function of m_H, when the TEVATRON value of m_t is used as an additional constraint in the fit. The observed $\Delta\chi^2$ curve exhibits a minimum for low values of m_H. The $\Delta\chi^2 = 2.7$ interval, approximately corresponding to a 95% confidence level upper limit, extends up to 500 GeV (850 GeV) including (excluding) the measurements of R_b and R_c.

7 Conclusions

The combination of the many precise electroweak results yields stringent constraints on the Standard Model. All LEP measurements except two agree well with the predictions. The measurements of the ratios of the b and c quark partial widths of the Z to its total hadronic width, dominated by systematic errors, are in rather poor agreement with the Standard Model. This has only a small effect on the predicted top-quark mass, which is in good agreement with the direct measurement of the top mass at the TEVATRON. Including this direct measurement, the data show some sensitivity to the Higgs mass.

The LEP experiments wish to stress that this report reflects a preliminary status at the time of the 1995 summer conferences. A definitive statement on these results has to wait for publication by each collaboration.

Acknowledgements

We would like to thank the SL Division of CERN for the efficient operation of the LEP accelerator, the precise information on the absolute energy scale and their close cooperation with the four experiments. We would also like to thank members of the CCFR, CDF, DØ and SLD Collaborations for making results available to us in advance of the conferences and for useful discussions concerning their combination. In particular, we would like to thank Su Dong, J. Huber and B. Schumm from the SLD Collaboration for providing us with a breakdown of the systematic uncertainties in their heavy flavour analyses in a form which allowed a consistent combination with the LEP results.

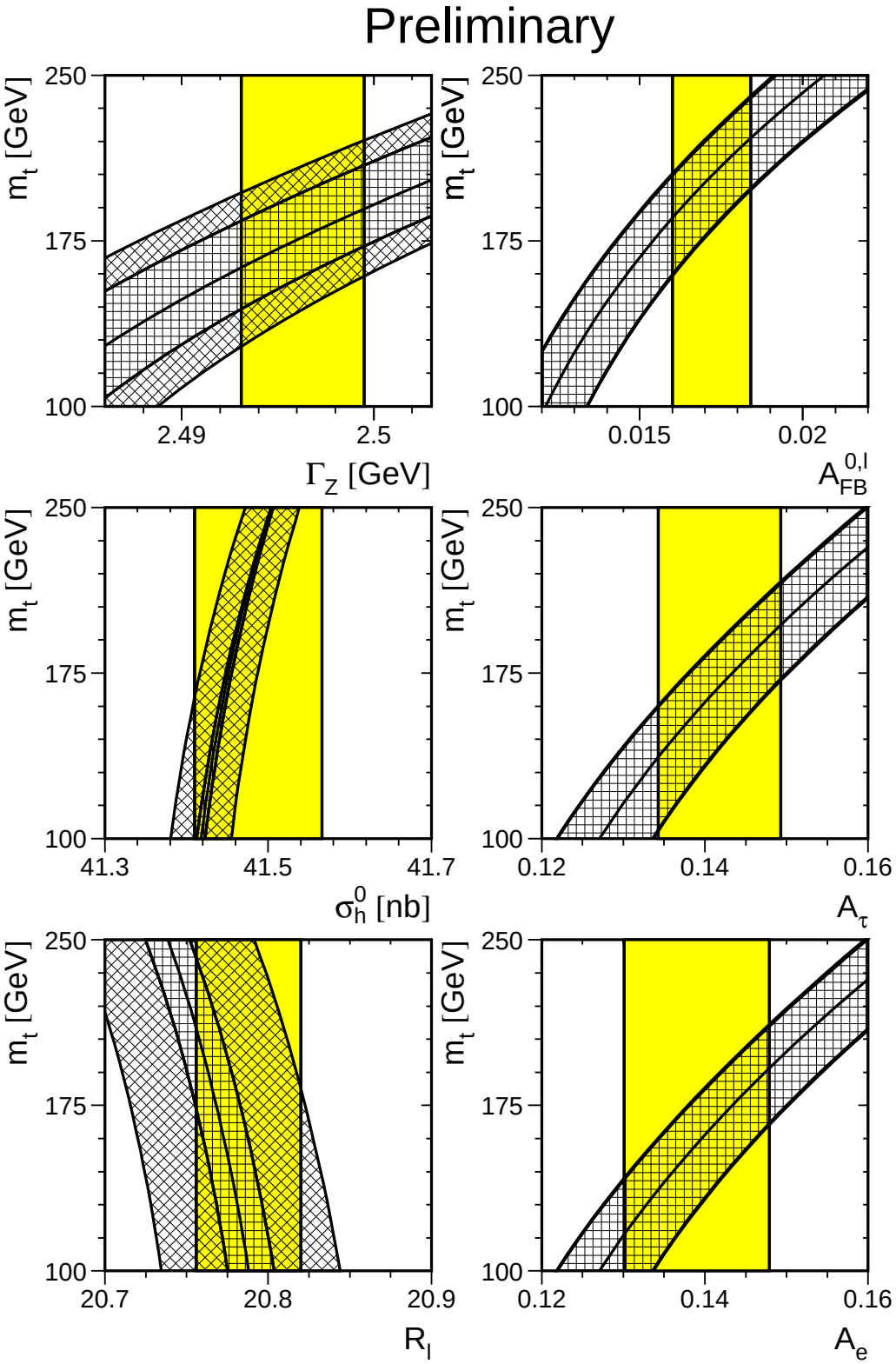

Figure 3: Comparison of LEP measurements with the Standard Model prediction as a function of m_t. The cross-hatch pattern parallel to the axes indicates the variation of the Standard Model prediction with m_H spanning the interval 60 GeV $\leq m_H \leq$ 1000 GeV, and the diagonal cross-hatch pattern corresponds to a variation of $\alpha_s(m_Z^2)$ within the interval $\alpha_s(m_Z^2) = 0.123 \pm 0.006$. The total width of the band corresponds to the linear sum of both uncertainties. The experimental errors on the parameters are indicated as vertical bands.

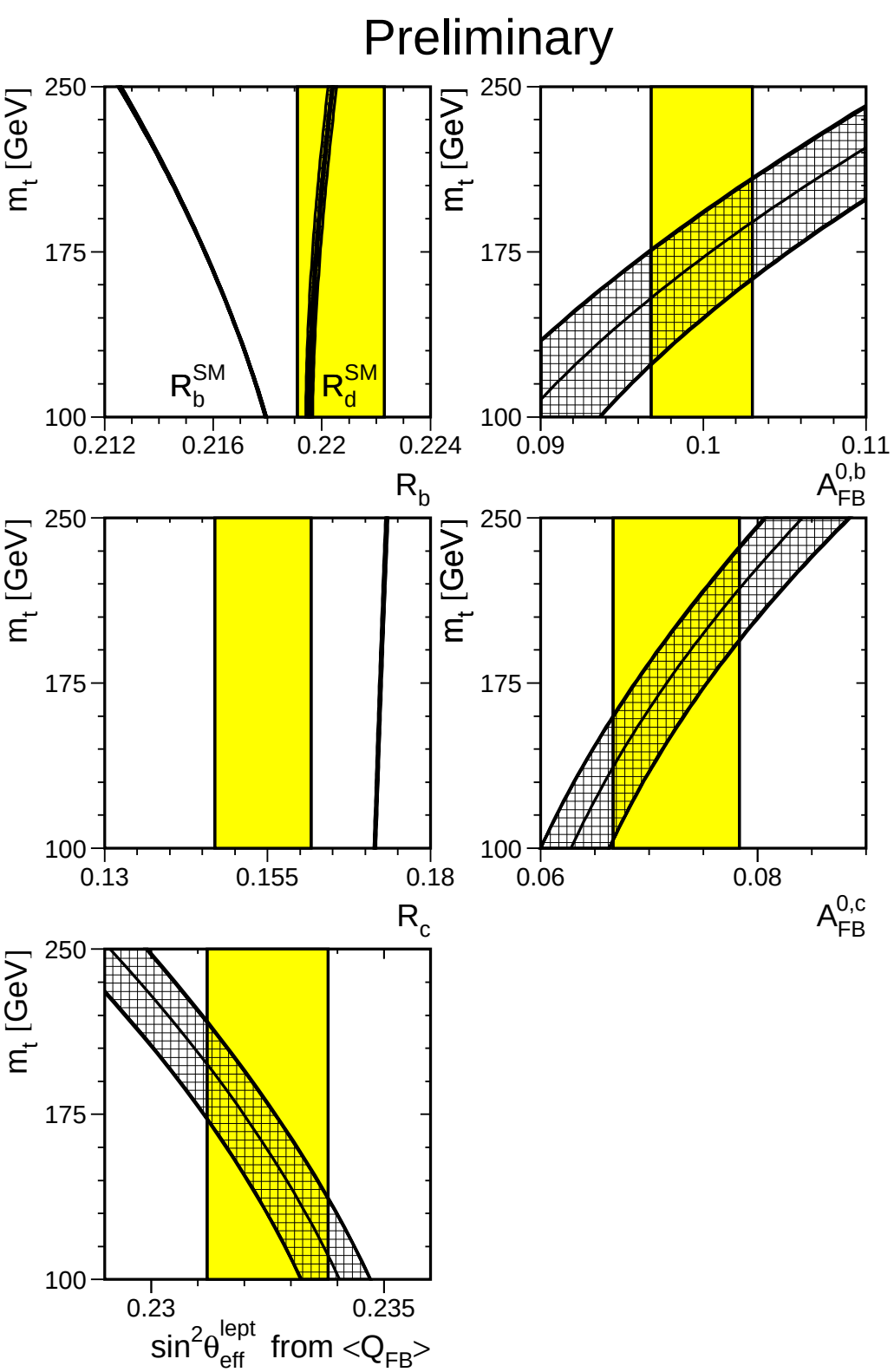

Figure 4: Comparison of LEP measurements with the Standard Model prediction as a function of m_t (*c.f.* Figure 3). For ratios of hadronic partial widths the variations with m_H and $\alpha_s(m_Z^2)$ nearly cancel. For the comparison of R_b with the Standard Model the value of R_c has been fixed to its Standard Model prediction. To illustrate the impact of special vertex corrections to R_b the Standard Model prediction for R_d is also indicated.

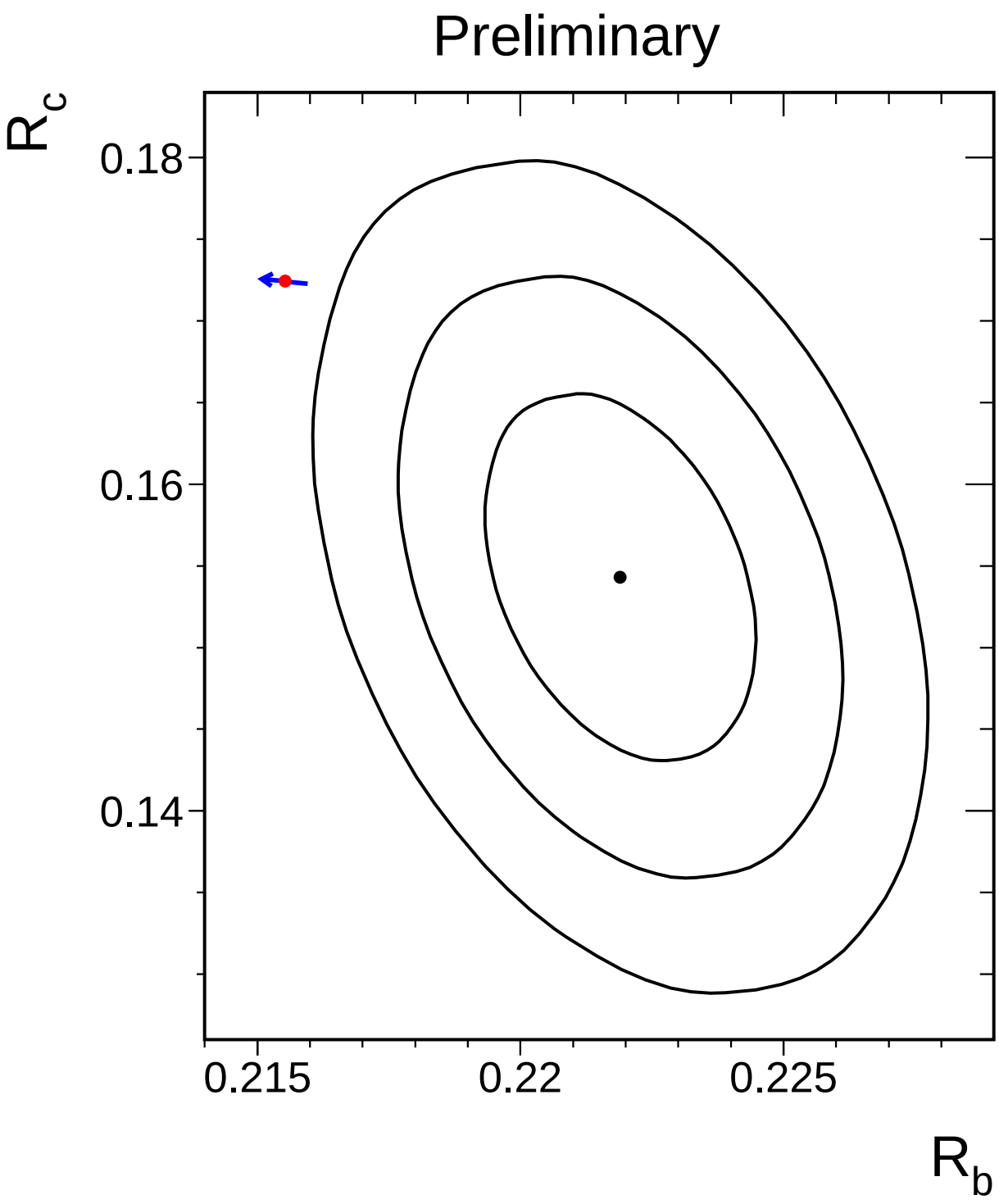

Figure 5: Contours in the R_b-R_c plane derived from LEP data, corresponding to 68%, 95% and 99.7% confidence levels assuming Gaussian systematic errors. The Standard Model prediction for $m_t = 180 \pm 12$ GeV is also shown. The arrow points in the direction of increasing values of m_t.

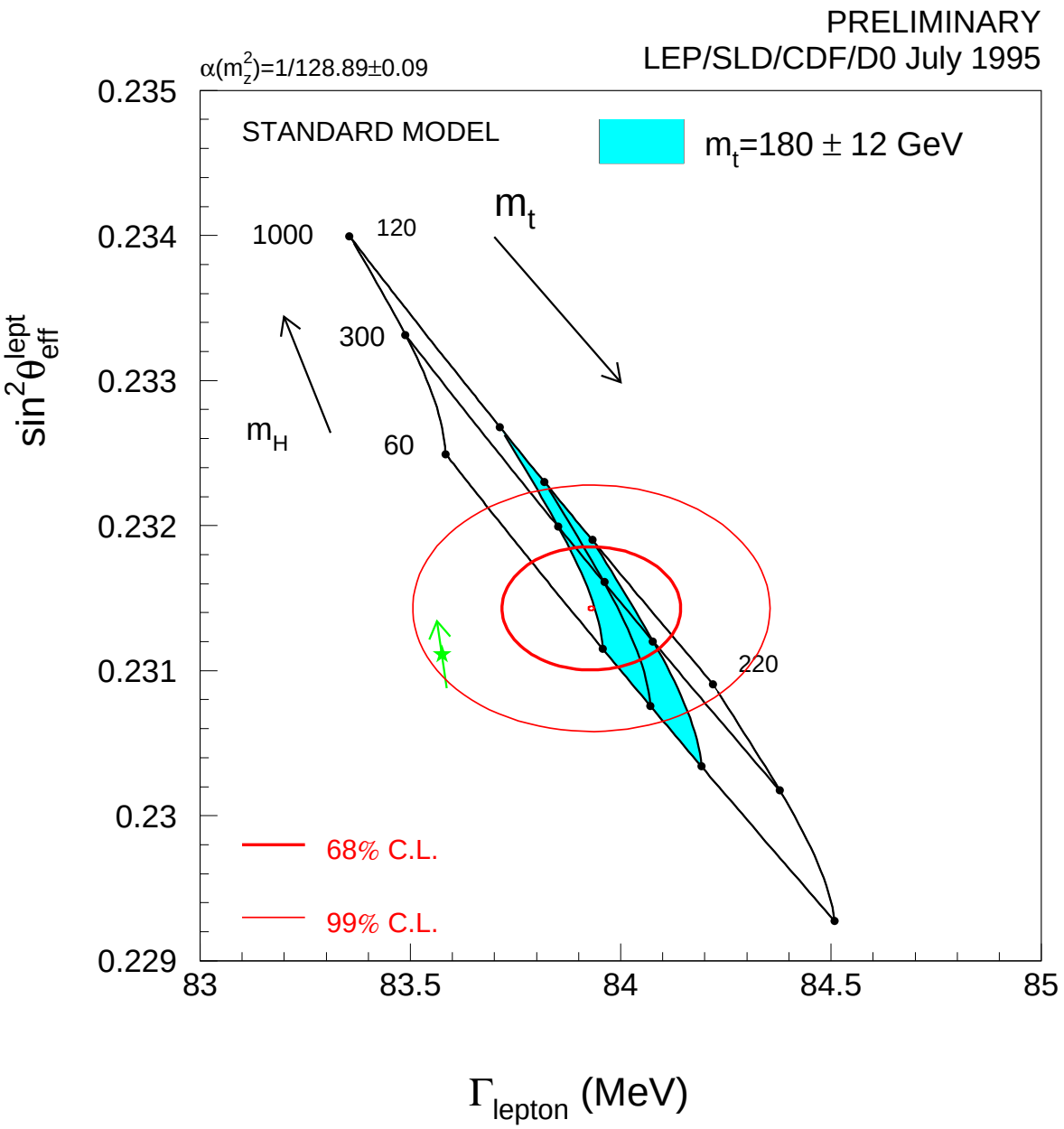

Figure 6: The LEP/SLD measurements of $\sin^2\theta^{\rm lept}_{\rm eff}$ (Table 21) and $\Gamma_{\ell\ell}$ (Table 9) and the Standard Model prediction. The star shows the predictions if among the electroweak radiative corrections only the photon vacuum polarization is included. The corresponding arrow shows variation of this prediction if $\alpha(m_{\rm Z}^2)$ is changing by one standard deviation. This variation gives an additional uncertainty to the Standard Model prediction shown in the figure.

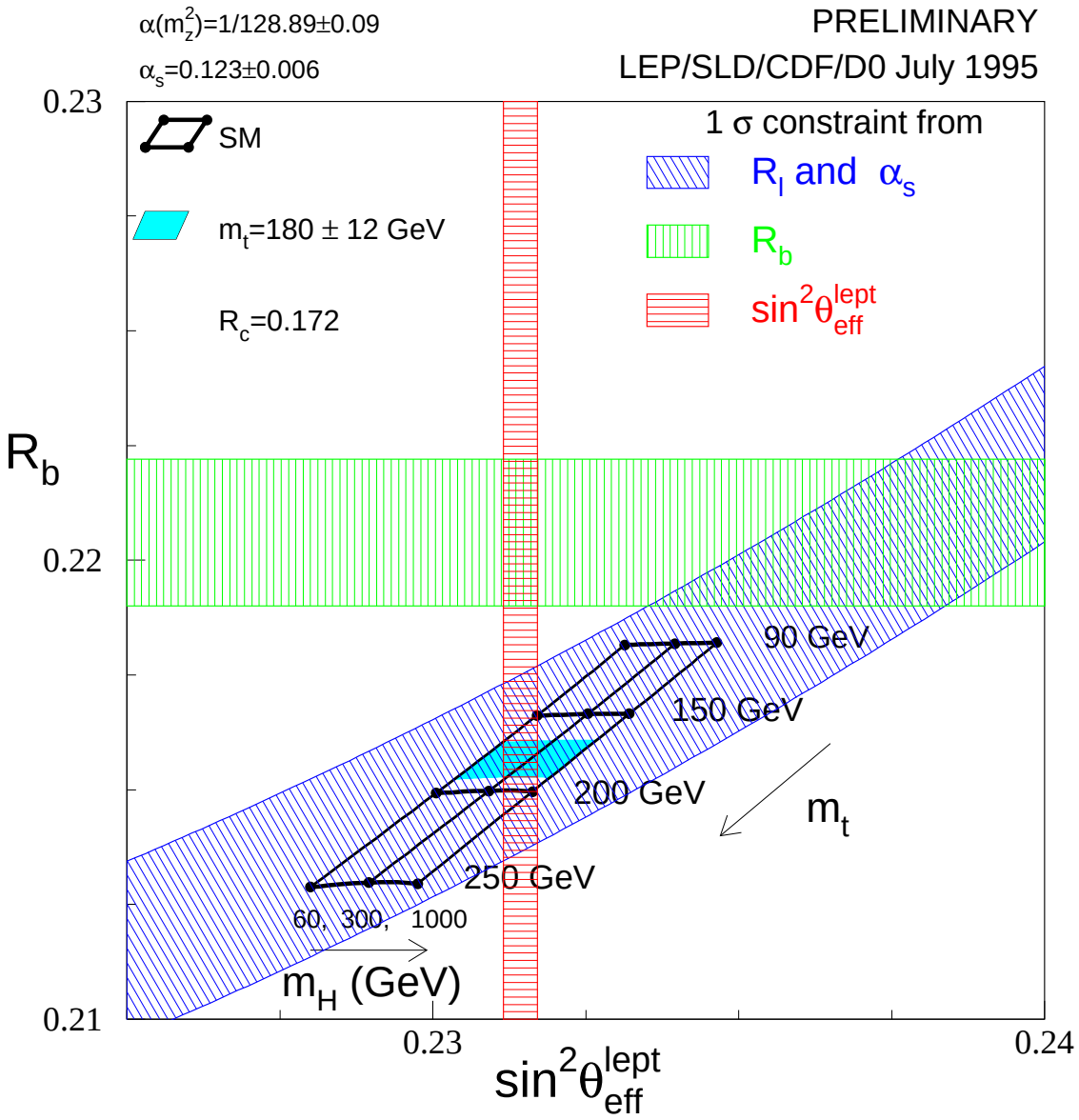

Figure 7: The LEP/SLD measurements of $\sin^2\theta^{\rm lept}_{\rm eff}$ (Table 21) and $R_{\rm b}(R_{\rm c} = 0.172)$ and the Standard Model prediction. Also shown is the constraint resulting from the measurement of R_ℓ on these variables, assuming $\alpha_s(m_{\rm Z}^2) = 0.123 \pm 0.006$, as well as the Standard Model dependence of light-quark partial widths on $\sin^2\theta^{\rm lept}_{\rm eff}$. The Standard Model value for $R_{\rm c}$ is assumed.

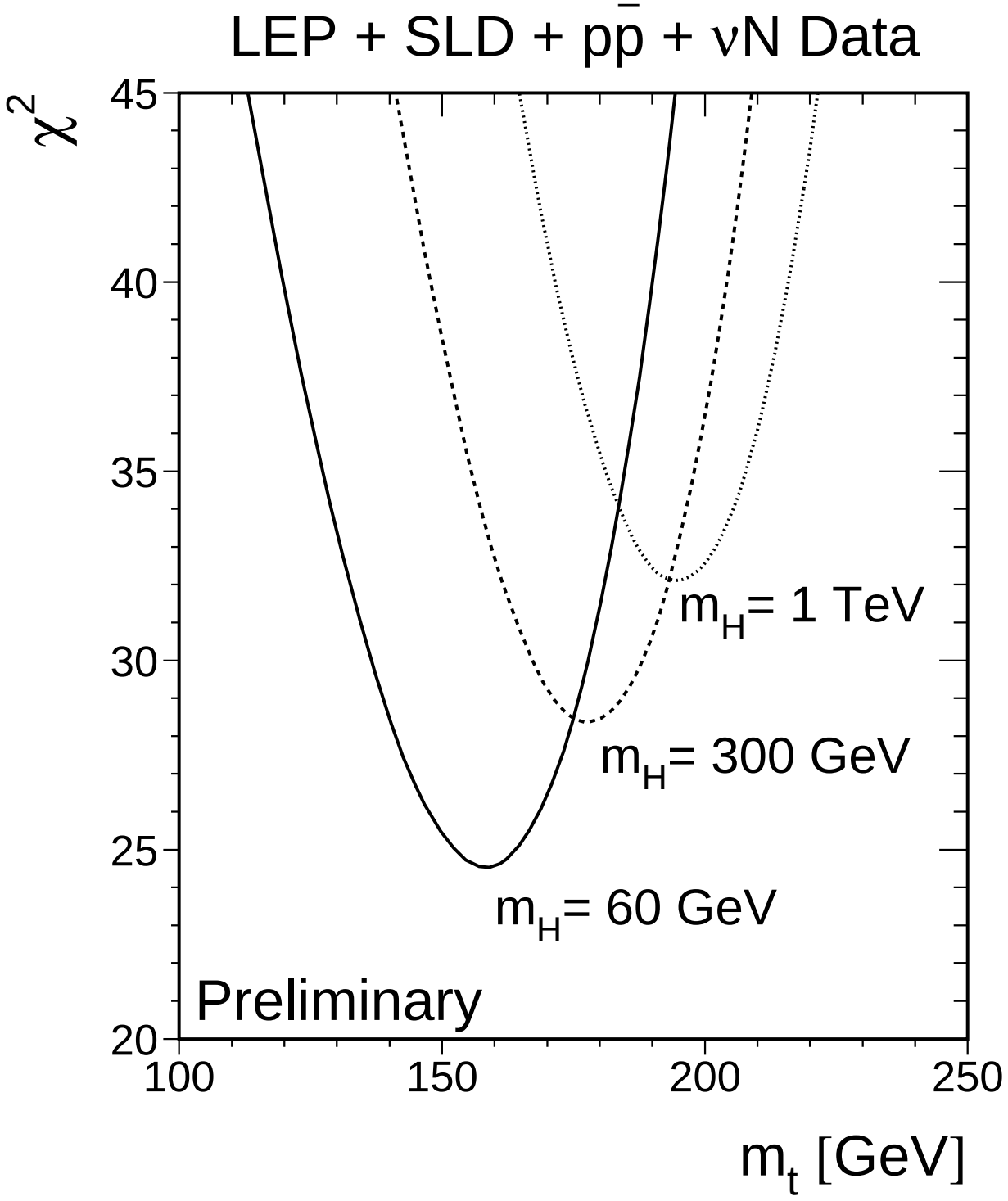

Figure 8: The χ^2 curves for the Standard Model fit in Table 23, column 4 to the electroweak precision measurements listed in Table 22 as a function of $m_{\rm t}$ for three different Higgs mass values spanning the interval 60 GeV $\leq m_{\rm H} \leq$ 1000 GeV.

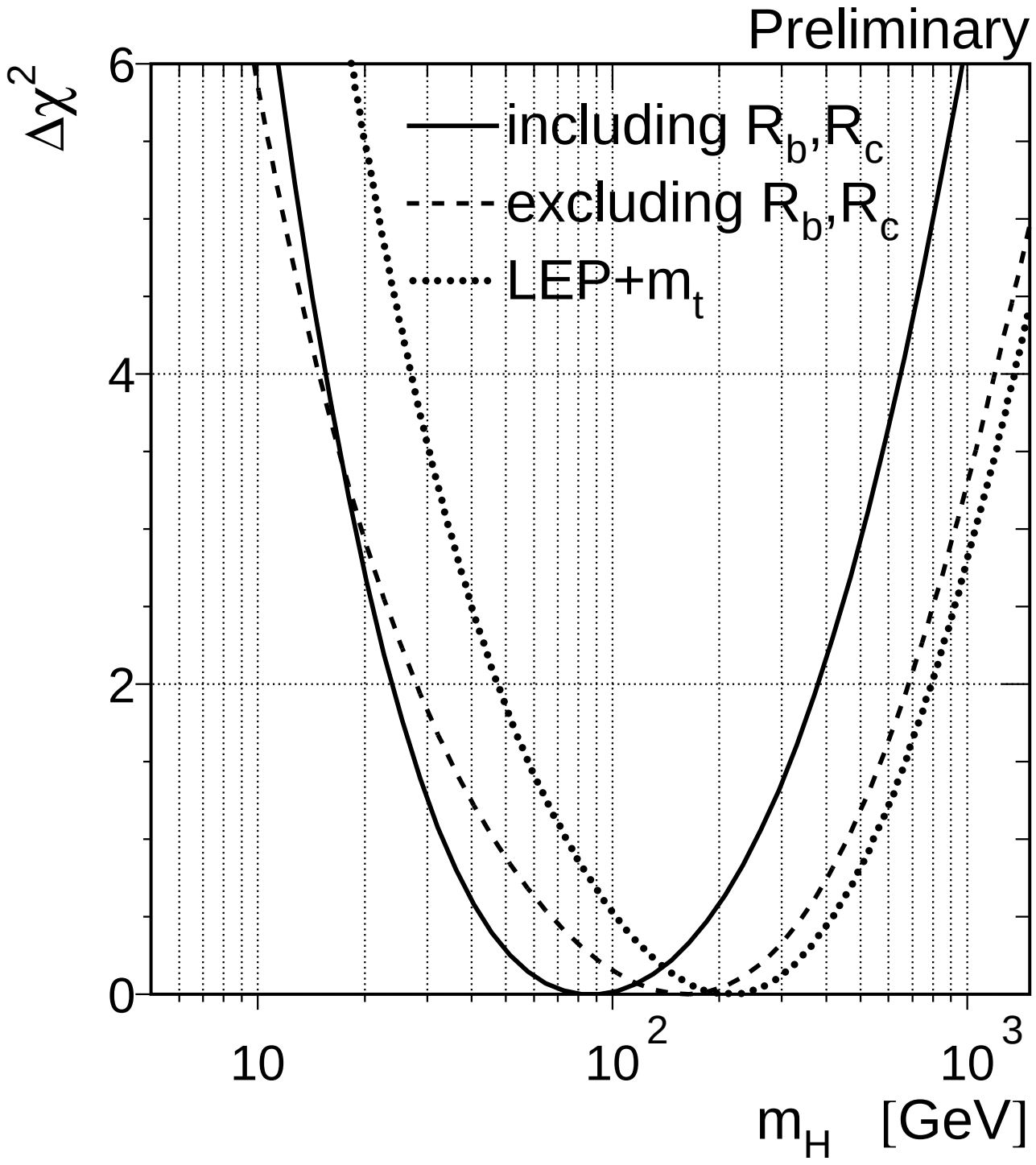

Figure 9: $\Delta\chi^2 = \chi^2 - \chi^2_{min}$ vs $m_{\rm H}$ curves. Continuous line: using all data (last column of Table 23); dashed line: as before, but excluding the LEP+SLD measurements of $R_{\rm b}$ and $R_{\rm c}$; dotted line: using LEP data (first column of Table 23) including the LEP measurements of $R_{\rm b}$ and $R_{\rm c}$. In all cases, the direct measurement of $m_{\rm t}$ at the TEVATRON is included.

Appendix

The Measurements used in the Heavy Flavour Averages

In the following tables, preliminary results are indicated by the symbol †. In each table, the values of centre-of-mass energy are given where relevant, followed by the result, the statistical error, the correlated and uncorrelated systematic errors, the total systematic error, and any dependence on other electroweak parameters. Contributions to the correlated systematic error are from any sources of error shared with one or more other results in the same table, and the uncorrelated errors from the remaining sources. Constants such as $a(x)$ denote the dependence on the assumed value of x^{used}, which is also given.

	ALEPH			DELPHI	
Tagging	90-91 shape [41]	90-91 lepton [36]	92 lifetime [43]	90-93† multiple [44]	91-92 lepton [37]
R_{b}	0.2280	0.2162	0.2187	0.2210	0.2145
Statistical	0.0054	0.0062	0.0022	0.0016	0.0089
Uncorrelated	0.0036	0.0028	0.0022	0.0013	0.0063
Correlated	0.0032	0.0042	0.0012	0.0015	0.0023
Total Systematic	0.0048	0.0050	0.0025	0.0020	0.0067
$a(R_{\text{c}})$	−0.004		−0.014	−0.015	
$R_{\text{c}}^{\text{used}}$	0.165		0.171	0.171	

	L3		OPAL		SLD
Tagging	91 shape [42]	90-91† lepton [39]	92-94† multiple [45]	90-91 lepton [40]	93-94† lifetime [13]
R_{b}	0.2220	0.2187	0.2197	0.2250	0.2171
Statistical	0.0030	0.0081	0.0014	0.0110	0.0040
Uncorrelated	0.0053	0.0047	0.0012	0.0035	0.0027
Correlated	0.0036	0.0034	0.0018	0.0057	0.0026
Total Systematic	0.0064	0.0058	0.0022	0.0066	0.0037
$a(R_{\text{c}})$	−0.021	−0.023	−0.018	−0.013	−0.023
$R_{\text{c}}^{\text{used}}$	0.171	0.171	0.171	0.171	0.171
$a(\text{BR}(\text{b} \to \ell))$	−0.001				
$\text{BR}(\text{b} \to \ell)^{\text{used}}$ [%]	10.5				
$a(\text{BR}(\text{b} \to \text{c} \to \bar{\ell}))$		0.034			
$\text{BR}(\text{b} \to \text{c} \to \bar{\ell})^{\text{used}}$ [%]		7.9			

Table 24: The measurements of R_{b}. There is an additional +0.2 statistical and +0.2 systematic correlation between the first two ALEPH results [36, 41].

	ALEPH	DELPHI			OPAL	
Tagging	90-91 lepton [36]	91-94† D inclusive [48]	91-93† D exclusive [48]	91-92 lepton [37]	90-94† $D^{*\pm}$ [49]	90-94† D^0, D^+, D_s, Λ_c [49]
R_c	0.1670	0.152	0.155	0.1625	0.146	0.162
Statistical	0.0054	0.010	0.009	0.0085	0.007	0.011
Uncorrelated	0.0149	0.010	0.009	0.0177	0.011	0.009
Correlated	0.0114	0.006	0.017	0.0111	0.007	0.010
Total Systematic	0.0188	0.016	0.019	0.0209	0.013	0.020

Table 25: The measurements of R_c.

	ALEPH			DELPHI		L3	OPAL		
Tagging	90-93 lepton [36]	90-93 lepton [36]	90-93 lepton [36]	91-94† lepton [38]	91-94† $D^{*\pm}$ [38]	90-93† lepton [39]	91-94 jet [47]	90-94† lepton [40]	90-94† $D^{*\pm}$ [51]
$\sqrt{s}$ (GeV)	88.36	89.42	90.21	89.43	89.54	89.56	89.52	89.54	89.54
$A_{FB}^{bb}(-2)$	−3.1	3.3	9.3	6.3	1.9	7.02	6.3	3.3	2.7
Statistical	11.0	3.0	5.8	3.8	10.5	3.50	3.4	3.0	16.9
Uncorrelated	0.0	0.0	0.0	0.2	1.1	0.35	0.2	0.7	3.8
Correlated	0.1	0.1	0.3	0.1	0.8	0.12	0.1	0.2	0.3
Total Systematic	0.1	0.1	0.3	0.2	1.4	0.37	0.2	0.8	3.8
$a(R_b)$				−0.007		−1.642	−1.8		
R_b^{used}				0.217		0.216	0.216		
$a(R_c)$				0.122		0.913	0.01	−0.658	
R_c^{used}				0.171		0.169	0.173	0.171	
$a(\overline{\chi})$				2.053					
$\overline{\chi}^{used}$				0.121					
$a(BR(b \to \ell))$				−0.971		−0.928			
$BR(b \to \ell)^{used}$ [%]				11.0		10.5			
$a(BR(b \to c \to \bar{\ell}))$				0.158		−0.066			
$BR(b \to c \to \bar{\ell})^{used}$ [%]				7.9		7.9			
$a(A_{FB}^{c\bar{c}}(-2))$						−0.267	−0.205		
$A_{FB}^{c\bar{c}}(-2)^{used}$						−2.9	−3.16		

Table 26: The measurements of $A_{FB}^{b\bar{b}}(-2)$ (in units of 10^{-2}).

	ALEPH		DELPHI			L3	OPAL		
Tagging	90-93 lepton [36]	91-93 jet [46]	91-94† jet [38]	91-94† lepton [38]	91-94† $D^{*\pm}$ [38]	90-93† lepton [39]	91-94† jet [47]	90-94† lepton [40]	90-94† $D^{*\pm}$ [51]
$\sqrt{s}$ (GeV)	91.26	91.19	91.23	91.23	91.23	91.27	91.25	91.24	91.20
$A_{\rm FB}^{\rm bb}({\rm pk})$	8.43	9.92	9.90	10.49	7.1	10.3	9.73	10.30	11.2
Statistical	0.68	0.84	0.72	0.76	2.5	1.0	0.67	0.90	3.5
Uncorrelated	0.08	0.25	0.28	0.19	1.1	0.4	0.23	0.24	1.7
Correlated	0.11	0.28	0.25	0.24	0.8	0.1	0.32	0.27	1.0
Total Systematic	0.14	0.38	0.38	0.31	1.4	0.4	0.39	0.36	2.0
$a(R_{\rm b})$		−3.07	−0.6	−2.893		−1.642	−10.09		
$R_{\rm b}^{\rm used}$		0.2188	0.221	0.217		0.216	0.216		
$a(R_{\rm c})$		+2.57	0.24	1.221		0.913	0.109	1.71	
$R_{\rm c}^{\rm used}$		0.171	0.171	0.171		0.169	0.173	0.171	
$a(\overline{\chi})$				3.447					
$\overline{\chi}^{\rm used}$				0.121					
$a({\rm BR}({\rm b}\to\ell))$				−3.559		−0.647			
${\rm BR}({\rm b}\to\ell)^{\rm used}$ [%]				11.0		10.5			
$a({\rm BR}({\rm b}\to{\rm c}\to\bar{\ell}))$				0.474		−0.283			
${\rm BR}({\rm b}\to{\rm c}\to\bar{\ell})^{\rm used}$ [%]				7.9		7.9			
$a(A_{\rm FB}^{\rm c\bar{c}}({\rm pk}))$						0.580	0.457		
$A_{\rm FB}^{\rm c\bar{c}}({\rm pk})^{\rm used}$						6.3	6.1		

Table 27: The measurements of $A_{\rm FB}^{\rm b\bar{b}}({\rm pk})$ (in units of 10^{-2}).

	ALEPH			DELPHI		L3	OPAL		
Tagging	90-93 lepton [36]	90-93 lepton [36]	90-93 lepton [36]	91-94† lepton [38]	91-94† $D^{*\pm}$ [38]	90-93† lepton [39]	91-94 jet [47]	90-94† lepton [40]	90-94† $D^{*\pm}$ [51]
$\sqrt{s}$ (GeV)	92.07	93.02	93.93	93.02	92.94	92.93	92.94	92.94	92.94
$A_{FB}^{b\bar{b}}(+2)$	5.1	10.5	11.8	14.9	5.6	11.0	17.3	12.1	−26.7
Statistical	4.9	2.4	7.5	3.6	9.6	2.9	2.9	2.7	14.0
Uncorrelated	0.0	0.0	0.0	0.5	1.1	0.4	0.6	0.6	4.0
Correlated	0.2	0.3	0.3	0.4	0.8	0.1	0.4	0.4	2.3
Total Systematic	0.2	0.3	0.3	0.6	1.4	0.4	0.7	0.7	4.6
$a(R_b)$				−2.893		−1.642	−18.32		
R_b^{used}				0.217		0.216	0.216		
$a(R_c)$				−0.977		0.913	0.157	2.631	
R_c^{used}				0.171		0.169	0.173	0.171	
$a(\overline{\chi})$				4.767					
$\overline{\chi}^{used}$				0.121					
$a(BR(b \to \ell))$				−3.235		−0.630			
$BR(b \to \ell)^{used}$ [%]				11.0		10.5			
$a(BR(b \to c \to \bar{\ell}))$				0.474		−0.303			
$BR(b \to c \to \bar{\ell})^{used}$ [%]				7.9		7.9			
$a(A_{FB}^{c\bar{c}}(+2))$						1.113	0.840		
$A_{FB}^{c\bar{c}}(+2)^{used}$						12.1	12.0		

Table 28: The measurements of $A_{FB}^{b\bar{b}}(+2)$ (in units of 10^{-2}).

	ALEPH	DELPHI	OPAL	
Tagging	91-94† $D^{*\pm}$ [50]	91-94† $D^{*\pm}$ [38]	90-94† lepton [40]	91-94† $D^{*\pm}$ [51]
$\sqrt{s}$ (GeV)	89.4	89.54	89.54	89.54
$A_{FB}^{c\bar{c}}(-2)$	−4.9	0.2	−21.1	−0.6
Statistical	7.6	5.2	4.8	6.8
Uncorrelated	0.8	0.6	2.9	1.2
Correlated	0.0	0.1	0.4	0.1
Total Systematic	0.8	0.6	2.9	1.2
$a(A_{FB}^{b\bar{b}}(-2))$	0.291			
$A_{FB}^{b\bar{b}}(-2)^{used}$	−1.7			
$a(R_c)$			11.97	
R_c^{used}			0.171	

Table 29: The measurements of $A_{FB}^{c\bar{c}}(-2)$ (in units of 10^{-2}).

	ALEPH		DELPHI		L3	OPAL	
Tagging	90-91 lepton [36]	91-94† $D^{*\pm}$ [50]	91-94† lepton [38]	91-94† $D^{*\pm}$ [38]	90-91 lepton [39]	90-94† lepton [40]	90-94† $D^{*\pm}$ [51]
$\sqrt{s}$ (GeV)	91.26	91.2	91.23	91.23	91.24	91.24	91.20
$A_{FB}^{c\bar{c}}(pk)$	9.1	6.4	8.37	7.5	7.8	5.2	6.8
Statistical	2.0	1.3	1.39	1.2	3.7	1.0	1.4
Uncorrelated	1.5	0.2	0.91	0.6	2.4	0.8	0.7
Correlated	1.0	0.2	0.74	0.1	0.6	0.8	0.1
Total Systematic	1.9	0.3	1.18	0.6	2.5	1.2	0.7
$a(R_b)$			3.617		4.32		
R_b^{used}			0.217		0.216		
$a(R_c)$			−6.351		−6.76	−3.815	
R_c^{used}			0.171		0.169	0.171	
$a(BR(b \to \ell))$			4.853		3.501		
$BR(b \to \ell)^{used}$ [%]			11.0		10.5		
$a(BR(b \to c \to \bar{\ell}))$			−3.792		−0.303		
$BR(b \to c \to \bar{\ell})^{used}$ [%]			7.9		7.9		
$a(A_{FB}^{b\bar{b}}(pk))$		−1.491			6.400		
$A_{FB}^{b\bar{b}}(pk)^{used}$		8.7			8.8		

Table 30: The measurements of $A_{FB}^{c\bar{c}}(pk)$ from D^* meson and lepton-tag analyses (in units of 10^{-2}).

	ALEPH	DELPHI	OPAL	
Tagging	91-94† $D^{*\pm}$ [50]	91-94† $D^{*\pm}$ [38]	90-94† lepton [40]	90-94† $D^{*\pm}$ [51]
$\sqrt{s}$ (GeV)	93.0	92.94	92.94	92.94
$A_{FB}^{c\bar{c}}(+2)$	10.9	8.0	9.0	17.1
Statistical	6.1	4.6	4.0	5.8
Uncorrelated	0.7	0.6	2.0	1.4
Correlated	0.3	0.1	0.2	0.1
Total Systematic	0.8	0.6	2.0	1.4
$a(A_{FB}^{b\bar{b}}(+2))$	−2.074			
$A_{FB}^{b\bar{b}}(+2)^{used}$	12.1			
$a(R_c)$			−4.735	
R_c^{used}			0.171	

Table 31: The measurements of $A_{FB}^{c\bar{c}}(+2)$ (in units of 10^{-2}).

	SLD		
Tagging	93-95† jet [12]	94-95† $K^{\pm}$ [12]	93-95† lepton [12]
$\sqrt{s}$ (GeV)	91.26	91.26	91.26
$\mathcal{A}_b$	0.843	0.907	0.865
Statistical	0.046	0.094	0.072
Uncorrelated	0.045	0.091	0.071
Correlated	0.020	0.013	0.017
Total Systematic	0.049	0.092	0.073
$a(R_b)$	−0.131	−0.022	−0.654
R_b^{used}	0.2180	0.2180	0.2180
$a(R_c)$	0.133	0.003	0.073
R_c^{used}	0.171	0.171	0.171
$a(\mathcal{A}_c)$	0.081	−0.133	
$\mathcal{A}_c^{used}$	0.666	0.666	
$a(\overline{\chi})$		0.223	0.020
$\overline{\chi}^{used}$		0.13	0.120
$a(BR(b \to \ell))$			−0.222
$BR(b \to \ell)^{used}$ [%]			10.8
$a(BR(b \to c \to \ell)$			0.064
$BR(b \to c \to \bar{\ell})^{used}$ [%]			9.3

Table 32: The measurements of $\mathcal{A}_b$.

	SLD	
Tagging	93-95† $D^{*\pm}$ [12]	93-95† lepton [12]
$\sqrt{s}$ (GeV)	91.26	91.26
$\mathcal{A}_c$	0.64	0.44
Statistical	0.11	0.11
Uncorrelated	0.05	0.08
Correlated	0.02	0.05
Total Systematic	0.06	0.10
$a(R_b)$		0.654
R_b^{used}		0.2180
$a(R_c)$		−0.452
R_c^{used}		0.171
$a(\mathcal{A}_b)$	−0.128	
$\mathcal{A}_b^{used}$	0.935	
$a(BR(b \to \ell))$		0.415
$BR(b \to \ell)^{used}$ [%]		10.8
$a(BR(b \to c \to \bar{\ell})$		−0.436
$BR(b \to c \to \bar{\ell})^{used}$ [%]		9.3

Table 33: The measurements of $\mathcal{A}_c$.

Tagging	ALEPH 90-91 lepton [36]	ALEPH 92-93† multiple [36]	DELPHI 91-92 lepton [37]	L3 90-91† lepton [39]	OPAL 90-91† lepton [40]
BR(b $\to \ell$)(%)	11.20	11.01	11.21	11.44	10.50
Statistical	0.33	0.10	0.45	0.48	0.60
Uncorrelated	0.32	0.20	0.50	0.37	0.39
Correlated	0.27	0.21	0.48	0.22	0.54
Total Systematic	0.42	0.29	0.70	0.43	0.66
$a(R_c)$				0.611	0.224
R_c^{used}				0.171	0.171
$a(\overline{\chi})$		0.208			
$\overline{\chi}^{used}$		0.1261			
a(BR(b $\to$ c $\to \bar{\ell}$)				0.461	
BR(b $\to$ c $\to \bar{\ell}$)^{used} [%]				7.9	

Table 34: The measurements of BR(b $\to \ell$) from the lepton-tag analyses.

Tagging	ALEPH 90-91 lepton [36]	ALEPH 92-93† multiple [36]	DELPHI 91-92 lepton [37]	OPAL 90-91† lepton [40]
BR(b $\to$ c $\to \bar{\ell}$) (%)	8.81	7.68	7.70	8.30
Statistical	0.25	0.18	0.49	0.40
Uncorrelated	0.40	0.25	0.95	0.57
Correlated	0.69	0.42	0.83	0.39
Total Systematic	0.80	0.49	1.26	0.69
$a(R_c)$				0.316
R_c^{used}				0.171
$a(\overline{\chi})$		-0.511		
$\overline{\chi}^{used}$		0.1261		

Table 35: The measurements of BR(b $\to$ c $\to \bar{\ell}$) from the lepton-tag analyses.

Tagging	ALEPH 90-91 lepton [36]	DELPHI 91-92 lepton [37]	L3 90-93† lepton [39]	OPAL 90-91† lepton [40]
$\overline{\chi}$	0.0993	0.1500	0.1253	0.1440
Statistical	0.0073	0.0200	0.0110	0.0220
Uncorrelated	0.0028	0.0107	0.0053	0.0055
Correlated	0.0051	0.0119	0.0025	0.0028
Total Systematic	0.0058	0.0160	0.0058	0.0062
$a(R_{\mathrm{b}})$			0.001	
$R_{\mathrm{b}}^{\mathrm{used}}$			0.216	
$a(R_{\mathrm{c}})$			0.001	0.013
$R_{\mathrm{c}}^{\mathrm{used}}$			0.169	0.171
$a(\mathrm{BR}(\mathrm{b} \to \ell))$			0.046	
$\mathrm{BR}(\mathrm{b} \to \ell)^{\mathrm{used}}$ [%]			10.5	
$a(\mathrm{BR}(\mathrm{b} \to \mathrm{c} \to \ell)$			−0.0342	
$\mathrm{BR}(\mathrm{b} \to \mathrm{c} \to \bar{\ell})^{\mathrm{used}}$ [%]			7.9	

Table 36: The measurements of $\overline{\chi}$ from the lepton-tag analyses.

References

[1] The LEP Collaborations ALEPH, DELPHI, L3, OPAL and the LEP Electroweak Working Group, *Combined Preliminary Data on* Z *Parameters from the LEP Experiments and Constraints on the Standard Model*, CERN-PPE/94-187.

[2] The working group on LEP energy, R. Assmann et al., Z. Phys. **C66** (1995) 567.

[3] S. Jadach, E. Richter-Wąs, B.F.L. Ward and Z. Wąs, Phys. Lett. **B353** (1995) 362.

[4] M. L. Swartz, *Reevaluation of the Hadronic Contribution to* $\alpha(M_Z^2)$, SLAC-PUB-6710, November 1994, SLAC-PUB-95-7001, September 1995.

[5] A.D. Martin and D. Zeppenfeld, Phys. Lett. **B345** (1994) 558.

[6] S. Eidelmann and F. Jegerlehner, Z. Phys. **C67** (1995) 585.

[7] H. Burkhardt and B. Pietrzyk, Phys. Lett. **B356** (1995) 398.

[8] CDF Collaboration, F. Abe *et al.*, Phys. Rev. Lett. **74** (1995) 2626.

[9] DØ Collaboration, S. Abachi *et al.*, Phys. Rev. Lett. **74** (1995) 2632.

[10] SLD Collaboration, K. Abe *et al.*, Phys. Rev. Lett **73** (1994) 25.

[11] M. Woods, *The SLD* $A_{\rm LR}$ *Result and Review of Weak Mixing Angle Results at LEP and SLC*, Talk given at the EPS-HEP-95 Conference, Brussels, to appear in the Proceedings.

[12] J. Huber, *Left-right Forward-backward Asymmetry for c and b Quarks*, Talk given at the EPS-HEP-95 Conference, Brussels, to appear in the Proceedings;
C. Prescott, *Physics results with polarized electrons from SLAC*, Talk given at the 17th International Symposium on Lepton-Photon Interactions, 10-15/8/1995, Beijing, China, to appear in the Proceedings.

[13] SLD Collaboration, *A Measurement of* R_b *using Lifetime Double Tag*, Contributed Paper to EPS-HEP-95 Brussels, **eps0222**.
D.G. Charlton, *Measurement of* R_b *with lifetime tags*, Talk given at the EPS-HEP-95 Conference, Brussels, to appear in the Proceedings.

[14] CDHS Collaboration, H. Abramowicz *et al.*, Phys. Rev. Lett. **57** (1986) 298;
CDHS Collaboration, A. Blondel *et al.*, Z. Phys. **C45** (1990) 361.

[15] CHARM Collaboration, J.V. Allaby *et al.*, Phys. Lett. **B177** (1986) 446;
CHARM Collaboration, J.V. Allaby *et al.*, Z. Phys.**C36** (1987) 611.

[16] CCFR Collaboration, C.G. Arroyo *et al.*, Phys. Rev. Lett. **72** (1994) 3452;
D. Harris, *CCFR Measurement of* R_ν *and a New Extraction of* $\sin^2\theta_W$, Talk given at the EPS-HEP-95 Conference, Brussels, to appear in the Proceedings.

[17] UA2 Collaboration, J. Alitti *et al.*, Phys. Lett. **B276** (1992) 354.

[18] CDF Collaboration, F. Abe *et al.*, Phys. Rev. Lett. **65** (1990) 2243 and Phys. Rev. **D43** (1991) 2070.

[19] CDF Collaboration, F. Abe *et al.*, *Measurement of the W Boson Mass*, FERMILAB-PUB-95/033-E and FERMILAB-PUB-95/035-1995.

[20] DØ Collaboration, preliminary result presented by C.K. Jung, Proceedings of the XXVII International Conference on High-Energy Physics, Glasgow, Scotland, 1994, Vol.II, Institute of Physics Publishing, Bristol and Philadelphia.

[21] ALEPH Collaboration, D. Decamp *et al.*, Z. Phys. **C48** (1990) 365;
ALEPH Collaboration, D. Decamp *et al.*, Z. Phys. **C53** (1992) 1;
ALEPH Collaboration, D. Buskulic *et al.*, Z. Phys. **C60** (1993) 71;
ALEPH Collaboration, D. Buskulic *et al.*, Z. Phys. **C62** (1994) 539;
ALEPH Collaboration, *Preliminary Results on Z Production Cross Section and Lepton Forward-Backward Asymmetries using the 1994 Data*, note ALEPH 95-084 PHYSIC 95-078, eps0398.

[22] DELPHI Collaboration, P. Aarnio *et al.*, Nucl. Phys. **B367** (1991) 511;
DELPHI Collaboration, P. Abreu *et al.*, Nucl. Phys. **B417** (1994) 3;
DELPHI Collaboration, P. Abreu *et al.*, Nucl. Phys. **B418** (1994) 403;
DELPHI Collaboration, DELPHI Note 95-62 PHYS 497, July 1995.

[23] L3 Collaboration, B. Adeva *et al.*, Z. Phys. **C51** (1991) 179;
L3 Collaboration, O. Adriani *et al.*, Phys. Rep. **236** (1993) 1;
L3 Collaboration, M. Acciarri *et al.*, Z. Phys. **C62** (1994) 551;
L3 Collaboration, L3 Electroweak Update for 1995 Brussels/Beijing, L3 Note 1809, July 14, 1995.

[24] OPAL Collaboration, G. Alexander *et al.*, Z. Phys. **C52** (1991) 175;
OPAL Collaboration, P.D. Acton *et al.*, Z. Phys. **C58** (1993) 219;
OPAL Collaboration, R. Akers *et al.*, Z. Phys. **C61** (1994) 19;
OPAL Collaboration, *A Preliminary Update of the* Z *Line Shape and Lepton Asymmetry Measurements with the 1993 and 1994 Data*, Contributed Paper to EPS-HEP-95 Brussels, **eps0292**;
OPAL Collaboration, *The Preliminary OPAL SiW luminosity analysis: Results for the 1994 Summer conferences*, OPAL Physics Note PN142, July 1994.

[25] M. Koratzinos private communication and minutes of the 64th meeting of the LEP energy calibration working group, 17 February 1995.

[26] The LEP Collaborations ALEPH, DELPHI, L3, OPAL and the LEP Electroweak Working Group, *Updated Parameters of the* Z *Resonance from Combined Preliminary Data of the LEP Experiments*, CERN-PPE/93-157.

[27] See, for example, M. Consoli *et al.*, in "Z Physics at LEP 1", CERN Report CERN 89-08 (1989), eds G. Altarelli, R. Kleiss and C. Verzegnassi, Vol. 1, p. 7.

[28] LEP Electroweak Working Group, *An Investigation of the Interference between Photon and Z-Boson Exchange*, Internal Note, LEPEWWG/LS/95-01, ALEPH 95-95 PHYSIC 95-87, DELPHI 95-138 PHYS 563, L3 Note 1812, OPAL Technical Note TN314, 1 August 1995.

[29] ALEPH Collaboration, D. Buskulic *et al.*, *Improved tau polarisation measurements*, CERN-PPE/95-023 (1995).

[30] DELPHI Collaboration, P. Abreu *et al.*, Z. Phys. **C67** (1995) 183.

[31] L3 Collaboration, O. Acciari *et al.*, Phys. Lett. **B341** (1994) 245;
L3 Collaboration, *A Preliminary Update of* A_τ *and* A_e *Using 1994 Data*, Contributed Paper to EPS-HEP Brussels, **eps0094**.
The 1994 data have been combined with the earlier data using a 100% correlation of the systematic errors.

[32] OPAL Collaboration, *Updated Measurement of the Tau Polarisation Asymmetry*, Contributed Paper to EPS-HEP Brussels, **eps0295**.

[33] LEP Electroweak Working Group, *Presentation of LEP Electroweak Heavy Flavour Analyses for Summer 1994 Conferences*, LEPHF/94-02, ALEPH Note 94-90, DELPHI 94-23/add, L3 Note 1613, OPAL Technical Note TN237.

[34] P. Renton, *Review of Experimental Results on Precision Tests of Electroweak Theories*, Talk given at the 17th International Symposium on Lepton-Photon Interactions, 10-15/8/1995, Beijing, China, to appear in the Proceedings; Oxford University preprint OUNP-95-20.
T. Behnke, *Production of charm and measurements of charm electroweak properties at the Z using D^* and D mesons*, Talk given at the EPS-HEP-95 Conference, Brussels, to appear in the Proceedings.
A. Passeri, *Forward-Backward asymmetry for heavy flavours using lifetime based tags*, Talk given at the EPS-HEP-95 Conference, Brussels, to appear in the Proceedings.

[35] LEP Electroweak Working Group, *Combined LEP and SLD Electroweak Heavy Flavour Results for summer 1995 Conferences*, LEPHF/95-02, ALEPH Note 95-091 PHYSIC 95-084, DELPHI 95-115 PHYS 550, L3 Note 1813, OPAL Technical Note TN313, SLAC-PUB 95/6569.

[36] ALEPH Collaboration, D. Buskulic *et al.*, Z. Phys. **C62** (1994) 179;
ALEPH Collaboration, $B^0\overline{B^0}$ *mixing and* $b\bar{b}$ *asymmetry from high-p_t leptons,* ALEPH 94-036, contributed paper to the La Thuile and Moriond Winter conferences, 1994;
ALEPH Collaboration, *Heavy Flavour Lepton Contribution for Summer 1994 Conferences,* ALEPH 94-123 PHYSIC 94-107;
ALEPH Collaboration., D. Buskulic *et al.*, *Measurement of the semileptonic b branching ratios from inclusive leptons in Z decays*, Contributed Paper to EPS-HEP-95 Brussels, **eps0404**.

[37] DELPHI Collab., P.Abreu et al., Z. Phys. **C66** (1995) 323.

[38] DELPHI Collaboration, P.Abreu *et al.*, Z. Phys **C65** (1995) 569;
DELPHI Collaboration, P.Abreu *et al.*, Z. Phys **C66** (1995) 341;
DELPHI Collaboration, *Measurement of the Forward-Backward Asymmetries of $e^+e^- \to Z \to b\bar{b}$ and $e^+e^- \to Z \to c\bar{c}$* Contributed Paper to EPS-HEP-95 Brussels, **eps0571**, DELPHI 95-87 PHYS 522.

[39] L3 Collaboration, O. Adriani *et al.*, Phys. Lett. **B292** (1992) 454;
L3 Collaboration, M. Acciarri *et al.*, Phys. Lett. **B335** (1994) 542;
L3 Collaboration, *Measurement of R_b and BR($b \to \ell X$) from b-quark semileptonic decays,* L3 Note 1449, July 16 1993;
L3 Collaboration, *L3 Results on $A_{FB}^{b\bar{b}}$, $A_{FB}^{c\bar{c}}$ and χ for the Glasgow Conference,* L3 Note 1624;
L3 Collaboration, *L3 Results on R_b and BR($b \to \ell$) for the Glasgow Conference,* L3 Note 1625.
The sign of the correlation coefficient arising from the b semileptonic decay model has been corrected [54].

[40] OPAL Collaboration, R. Akers *et al.*, Z. Phys. **C60** (1993) 199;
OPAL Collaboration, *Measurement of the forward-backward asymmetries of* $e^+e^- \to Z \to b\bar{b}$ *and* $e^+e^- \to Z \to c\bar{c}$ *from events tagged by a lepton, including 1994 data*, Contributed Paper to EPS-HEP-95 Brussels, **eps0279**.

[41] ALEPH Collaboration, D. Buskulic *et al.*, Phys. Lett. **B313** (1993) 549.

[42] L3 Collaboration, O. Adriani *et al.*, Phys. Lett. **B307** (1993) 237.

[43] ALEPH Collaboration, D. Buskulic *et al.*, Phys. Lett. **B313** (1993) 535.

[44] DELPHI Collaboration, *Measurement of the partial decay width $R_b = \Gamma_{b\bar{b}}/\Gamma_{had}$ with the DELPHI detector at LEP* , Contributed Paper to EPS-HEP-95 Brussels, **eps0570**.

[45] OPAL Collaboration, Z. Phys. **C65** (1995) 17-30;
An Update of the Measurement of $\Gamma_{b\bar{b}}/\Gamma_{had}$ *using a Double Tagging Method*, Contributed Paper to EPS-HEP-95 Brussels, **eps0278**, OPAL Physics Note PN181.

[46] ALEPH Collaboration, D. Buskulic *et al.*, Phys. Lett. **B335** (1994) 99.

[47] OPAL Collaboration, R. Akers *et al.*, Z. Phys. **C67** (1995) 365.

[48] DELPHI Collaboration, *Study of Charm Mesons Production in Z^0 Decays and Measurement of* Γ_c/Γ_h Contributed Paper to EPS-HEP-95 Brussels, **eps0557**, DELPHI 95-101 PHYS 536.

[49] OPAL Collaboration, R. Akers *et al.*, Z. Phys. **C67** (1995) 27;
OPAL Collaboration, *A measurement of* $B(c \to D^*)$ *and* $\Gamma_{c\bar{c}}/\Gamma_{had}$ *using a double tagging technique*, Contributed Paper to EPS-HEP-95 Brussels, **eps0289**, OPAL physics note PN 175;
OPAL Collaboration, *A summary of OPAL measurements of charm production in* Z *decays*, OPAL Physics note PN190.

[50] ALEPH Collaboration, D. Buskulic *et al.*, Z. Phys. **C62** (1994) 1;
ALEPH Collaboration, D. Buskulic *et al.*, *The Forward–Backward Asymmetry for Charm Quarks at the Z pole: an Update*, Contributed Paper to EPS-HEP-95 Brussels, **eps0634**.

[51] OPAL Collaboration, *A Measurement of the Charm and Bottom Forward-Backward Asymmetry using D Mesons with the OPAL Detector at LEP* Contributed Paper to EPS-HEP-95 Brussels, **eps0290**, OPAL Physics Note, PN183.

[52] LEP Electroweak Working Group, *A Consistent Treatment of Systematic Errors for LEP Electroweak Heavy Flavour Analyses*, LEPHF/94-01, ALEPH Note 94-30, DELPHI 94-23 Phys 357, L3 Note 1577, OPAL Technical Note TN213.

[53] LEP Electroweak Working Group, *LEP Electroweak Heavy Flavour Results for Summer 1994 Conferences*, LEPHF/94-03, ALEPH Note 94-119 PHYSIC 94-103, DELPHI 94-108 PHYS 425, L3 Note 1630, OPAL Technical Note TN242.

[54] LEP Electroweak Working Group, *LEP Electroweak Heavy Flavour Results for Winter 1995 Conferences*, LEPHF/95-01, ALEPH Note 95-037 PHYSIC 95-035, DELPHI 95-28 PHYS 479, L3 Note 1735, OPAL Technical Note TN283.

[55] D. Bardin *et al.*, Z. Phys. **C44** (1989) 493; Comp. Phys. Comm. **59** (1990) 303; Nucl. Phys. **B351**(1991) 1; Phys. Lett. **B255** (1991) 290 and CERN-TH 6443/92 (May 1992).

[56] A. Djouadi, B. Lampe and P.M. Zerwas, Z. Phys. **C67** (1995) 123.

[57] ALEPH Collaboration, D. Decamp *et al.*, Phys. Lett. **B259** (1991) 377.

[58] ALEPH Collaboration, ALEPH-Note 93-041 PHYSIC 93-032 (1993);
ALEPH Collaboration, ALEPH-Note 93-042 PHYSIC 93-034 (1993);
ALEPH Collaboration, ALEPH-Note 93-044 PHYSIC 93-036 (1993).

[59] ALEPH Collaboration, *Jet charge measurements in $Z \to q\bar{q}$ decays*, Contributed Paper to EPS-HEP-95 Brussels, **eps0449**.

[60] DELPHI Collaboration, P. Abreu *et al.*, Phys. Lett. **B277** (1992) 371.

[61] OPAL Collaboration, P. D. Acton *et al.*, Phys. Lett. **B294** (1992) 436.

[62] OPAL Collaboration, OPAL Physics Note PN195 (1995).

[63] T. Sjöstrand, Comp. Phys. Comm. **82** (1994) 74.

[64] G. Marchesini *et al.*, Comp. Phys. Comm. **67** (1992) 465.

[65] CHARM II Collaboration, P. Vilain *et al.*, Phys. Lett. **B335** (1994) 246.

[66] S. Bethke, Proceedings of the QCD '94 Conference, Montpellier, France, Nucl. Phys. B. (Proc. Suppl.) **39B,C** (1995) 198.

[67] *Reports of the working group on precision calculations for the Z resonance*, eds. D. Bardin, W. Hollik and G. Passarino, CERN Yellow Report 95-03, Geneva, 31 March 1995.

[68] Electroweak libraries:
ZFITTER: see Reference 55;
BHM: G. Burgers, W. Hollik and M. Martinez; M. Consoli, W. Hollik and F. Jegerlehner: Proceedings of the Workshop on Z physics at LEP I, CERN Report 89-08 Vol.I,7 and G. Burgers, F. Jegerlehner, B. Kniehl and J. Kühn: the same proceedings, CERN Report 89-08 Vol.I, 55.
These computer codes have recently been upgraded by including the results of [67] and references therein.

[69] T. Hebbeker, M. Martinez, G. Passarino and G. Quast, Phys. Lett. **B331** (1994) 165.

[70] The average for m_{W} has been obtained taking into account the measurements [17–20]. The method of the combination follows the description in [72] treating the uncertainty due to parton distribution functions as the only common error. The measurements are averaged weighted by their uncorrelated uncertainties. The largest parton distribution function uncertainty quoted, $\Delta m_{\mathrm{W}} = 0.085$ GeV [17], is added to the uncorrelated error.

[71] A. Blondel and C. Verzegnassi, Phys. Lett. **B311** (1993) 346.

[72] M. Demarteau *et al.*, *Combining W Mass Measurements*, CDF/PHYS/CDF/PUBLIC/2552 and DØ NOTE 2115.